



UNIVERSIDADE D
COIMBRA

José Pedro Oliveira Andrade

**IMPLEMENTATION AND TESTING OF AN ACTIVE
INTELLIGENT BARRIER SYSTEM FOR
WILDFIRES**

**Dissertação no âmbito do Mestrado Integrado em Engenharia Mecânica, no ramo
de Energia e Ambiente orientada pelo Professor Doutor Domingos Xavier
Filomeno Carlos Viegas e pelo Professor Doutor Carlos Xavier Pais Viegas e
apresentada ao Departamento de Engenharia Mecânica da Faculdade de Ciências
e Tecnologia da Universidade de Coimbra.**

Setembro de 2019

1 2



9 0

FACULDADE DE
CIÊNCIAS E TECNOLOGIA
UNIVERSIDADE DE
COIMBRA

Implementation and testing of an active intelligent barrier system for wildfires

Submitted in Partial Fulfilment of the Requirements for the Degree of Master in Mechanical Engineering in the speciality of Energy and Environment

Implementação e teste de um sistema inteligente e ativo de barreiras contra fogos rurais

Author

José Pedro Oliveira Andrade

Advisors

Domingos Xavier Filomeno Carlos Viegas

Carlos Xavier Pais Viegas

Jury

President	Professor Doutor José Manuel Baranda Ribeiro Professor Auxiliar da Universidade de Coimbra Professor Doutor Gilberto Cordeiro Vaz
Vowel	Professor Adjunto do Instituto Superior de Engenharia de Coimbra
Advisor	Professor Doutor Carlos Xavier Pais Viegas Professor Auxiliar da Universidade de Coimbra

Institutional Collaboration



Associação para o
Desenvolvimento da
Aerodinâmica
Industrial



Centro de Estudos
sobre Incêndios
Florestais

Coimbra, September, 2019

And so now I'd like to say - people can change anything they want to. And that
means everything in the world.

Joe Strummer

Aos meus pais.

ACKNOWLEDGEMENTS

Thanks to Professor Xavier Viegas for his incredible work and initiative but also for all the teachings.

Also, a special thanks to Professor Carlos Viegas for his patience and availability but also for his ideas and advices.

This work was only possible because of the support of the ADAI/CEIF Team. Thanks to the entire team for the help with the laboratory tests. Also, thanks to Sr. Cardoso for the patience, the conversations and the help with the making of the pieces required to make this work.

On the other hand, a big thanks to my parents and family for all the help, understanding, trust and love shown through these years. Also, thanks to my grandparents, for the comfort, love and for showing me that there is always a solution for everything.

A special thanks to all my friends in Coimbra and Bragança, that I will not be able to enumerate, with the risk of forgetting important people. A big thanks to all of them. Thanks to Mariana, for all the support, help and understanding.

Also, thanks to my brothers in Johnny's Grace, for giving me some of my best days during this journey.

Abstract

Over time, but especially more recently, Portugal has been plagued by forest fires, with major impacts at various levels, whether destruction of landscapes, housing, loss of human lives, are some of the tragedies caused by forest fires. One strategy to address this calamity is the development of fire protection systems. This is where the Fireprotect project emerges, in which this work is inserted.

The work developed in this dissertation is part of one of these protection systems. It is a system of thermal barriers that aims to create security perimeters around the elements to be protected, and those can be houses, workplaces, land, etc., providing a double barrier composed of a fireproof screen based on fiberglass to stop the advance of the flame and protect it from radiation effects, and a water sprinkler system to humidify the surrounding terrain and the fabric itself. These barriers are modular, allowing multiple units to be coupled.

This system consists of an articulated structure that is coupled to a tower and that needs mechanisms to be extended and retracted, mechanisms whose development constitutes one of the objectives of this work. The strategy used consisted of a system of stepper motors and actuators controlled by a Wi-Fi electronic board, all of which are inside the tower.

The articulated structure was also implemented and a new approach to it was proposed, by changing the shape of the vertical support bars, in order to guarantee more stability. To assemble the system, several custom-made parts were used.

One of the most important factors in the success of the barriers is their ability to sustain wind force. For this, calculations were performed that allowed to obtain the structure dimensions in order to withstand the wind force.

The structure was then tested on a wind tunnel to evaluate how it reacted when subjected to air flow velocities of 1, 2, 3 and 4 m / s.

Finally, as the X-bars that made up the articulated structure were easily bendable, which caused stability problems, there was the need to make some shape optimization through computer simulation tests. These were intended to suggest new geometries for the bars, in order to guarantee them greater stability, in this case, circular and square section

bars. The displacements that the different solutions suffered when subjected to compressive forces were calculated.

Both laboratory tests and simulation tests served to draw some conclusions. Some suggestions were also left for future work in order to improve this protection system.

Keywords Forest Fires, Protection Systems, Thermal Barriers, Fireproof Fabric, Articulated Structure.

Resumo

Ao longo dos tempos, mas sobretudo mais recentemente, Portugal tem sido assolado por fogos florestais, com grandes impactos a vários níveis, sejam eles destruição de paisagens, de habitações, perdas de vidas humanas, são algumas das tragédias causadas pelos fogos florestais. Uma estratégia para fazer face a esta calamidade passa pelo desenvolvimento de sistemas de proteção de elementos expostos ao fogo. É neste âmbito que surge o projeto Fireprotect, no qual este trabalho está inserido.

O trabalho desenvolvido nesta dissertação faz parte de um destes sistemas de proteção. Trata-se de um sistema de barreiras térmicas que têm como objetivo a criação de perímetros de segurança em torno dos elementos a proteger, sejam eles casas, locais de trabalho, terrenos etc., providenciando uma barreira dupla composta por uma tela ignífuga à base de fibra de vidro para travar o avanço das chamas e proteger dos efeitos radiativos, e por um sistema de aspersão de água para a humedificação do terreno em volta e da própria tela. Estas barreiras são modulares, permitindo que várias unidades sejam acopladas.

Este sistema é composto por uma estrutura articulada que se encontra acoplada a uma torre e que necessita de mecanismos para ser estendida e recolhida, mecanismos esses cujo desenvolvimento constitui um dos objetivos deste trabalho. A estratégia usada consistiu num sistema de motores stepper e atuadores controlados através de uma placa eletrónica Wi-Fi, sendo que todos estes elementos se encontram dentro da torre.

Foi também realizada a implementação da estrutura articulada e proposta uma nova abordagem à mesma, através da alteração do formato das barras de suporte verticais, de modo a garantir-lhe mais estabilidade. Para proceder à montagem do sistema, foram usadas várias peças feitas por medida.

Um dos fatores mais importantes para o sucesso das barreiras é a sua capacidade de sustentação quando sujeitas a vento. Para isso foram também realizados cálculos que permitiram obter as dimensões da estrutura de forma a suportar a força do vento.

De seguida a estrutura foi testada em túnel de vento, para verificar como reagia quando sujeita a velocidades de ar de 1,2,3 e 4 m/s.

Por último, verificando-se que as barras em X que compunham a estrutura articulada dobravam facilmente, o que causava problemas de estabilidade, surgiu a necessidade de realizar a otimização da geometria da estrutura através de testes de simulação em computador. Estes tiveram como objetivo sugerir novas geometrias para as barras, de modo a garantir-lhes maior estabilidade, no caso, barras de secção circular e de secção quadrada. Foram calculados os deslocamentos que as diferentes soluções sofriam quando sujeitas a forças de compressão.

Tanto os ensaios laboratoriais como os testes de simulação serviram para tirar algumas conclusões. Foram também deixadas algumas sugestões para trabalhos futuros, com o objetivo de aperfeiçoar este sistema de proteção.

Palavras-chave: Fogos Florestais, Sistemas de Proteção, Barreiras Térmicas, Tela Ignífuga, Estrutura Articulada.

Contents

LIST OF FIGURES	xiii
LIST OF TABLES	xvi
LIST OF ACRONYMS/ ABBREVIATIONS.....	xviii
Acronyms/Abbreviations.....	xviii
1. INTRODUCTION	1
1.1. Motivation.....	4
1.2. Objectives	5
1.3. State of the art	6
2. Methodology.....	11
2.1. Hardware.....	11
2.1.1. Controller Board	11
2.1.2. Actuators.....	12
2.1.3. Cooling Fan	12
2.1.4. Power Supply.....	13
2.2. Software	14
2.2.1. User interface and communication	14
2.2.2. Programming	15
2.3. Structure Implementation	16
2.3.1. Airflow Resistance	24
3. Tests.....	29
3.1. Laboratory Tests	29
3.1.1. Methodology.....	29
3.1.2. Results	30
3.1.3. Discussion.....	35
3.2. Simulation Tests	36
3.2.1. Methodology.....	36
3.2.2. Results	38
3.2.3. Discussion.....	39
4. Conclusions	41
4.1. Achievements.....	41
4.2. Future Work.....	41
BIBLIOGRAPHY	44
ANNEX A	46
APPENDIX A	50

LIST OF FIGURES

Figure 1.1. Occurrences and Burned Area in Mainland Portugal, per year, between 1990 and 2019 - Data from SGIF database.	2
Figure 1.2. Distribution of burned areas in Mainland Portugal – October 31 st – Data from the 10th interim report of forest fires – 2017	3
Figure 1.3. CAD design of the barrier.	4
Figure 1.4. Fireprotect project logo.	5
Figure 1.5. Drawings of Teruel’s (2009) work.....	6
Figure 1.6. Drawings of Linares’ (2014) work.....	7
Figure 1.7. Drawings of Roger and Holliday’s (2004) work.....	8
Figure 1.8. Firemaster Plus ² Fire Curtain Barrier by Coopers.	8
Figure 1.9. Firemaster Concertina™ “Open” Active Fire Curtain Barrier Assemblies by Coopers.....	9
Figure 2.1. Duet 2 Wifi.....	11
Figure 2.2. C-Beam XL Nema 23 Actuator.	12
Figure 2.3. Controller board with the fan.	12
Figure 2.4. Power Supply.	13
Figure 2.5. Step Down Converter.	14
Figure 2.6. Print Screen of the software.	15
Figure 2.7. Generic G-Code Example.	15
Figure 2.8. Example of a G-Code.....	16
Figure 2.9. Scheme of the directions of the motors. The letter a represents the motors and the letter b represents the actuators.	16
Figure 2.10. Spacer separating the bars.....	17
Figure 2.11. Axle for the wheels.	17
Figure 2.12. First assembly of the structure.	18
Figure 2.13. Narrower vertical bar.	18
Figure 2.14. Wider vertical bar.....	19
Figure 2.15. Old approach (on the left) and new approach (on the right).	19
Figure 2.16. Detail of the new approach of the vertical supports.....	20
Figure 2.17. Pieces used to space bars.....	20
Figure 2.18. Pieces applied on the structure.....	21

Figure 2.19. X bars. 22

Figure 2.20. Fabric cut. 23

Figure 2.21. Final extended structure. 24

Figure 2.22. Closed structure. 24

Figure 2.23. Schemes used for the calculations. 25

Figure 2.24. Structure width versus wind speed (new approach). 27

Figure 2.25. Structure width versus wind speed (old approach). 27

Figure 3.1. Fully extended structure on the wind tunnel. 29

Figure 3.2. Positions of the cameras. 30

Figure 3.3. Initial position of the structure. 31

Figure 3.4. Representation for every air flow velocity. 31

Figure 3.5. Lines representing all the positions of the structure. 32

Figure 3.6. Initial position of the structure. 33

Figure 3.7. Representation for every air flow velocity. 34

Figure 3.8. Lines representing all the positions of the structure. 34

Figure 3.9. Structure displacement as a function of air flow velocity. 35

Figure 3.10. Fixtures (on the left) and loads (on the right) applied on an articulated bar... 36

Figure 3.11. Fixtures (on the left) and loads (on the right) applied on a bar with circular section. 37

Figure 3.12. Fixtures (on the left) and loads (on the right) applied on a bar with square section. 37

Figure 3.13. Displacements of the articulated bar. 38

Figure 3.14. Displacements of the circular section bar. 38

Figure 3.15. Displacements of the square section bar. 39

Figure A.1. DUET 2 Wifi Technical Specifications. 46

Figure A.2. C-Beam XL Nema 23 Technical Specifications. 47

Figure A.3. COOLER MASTER - Sickle Flow 120mm Blue LED Fan Technical Specifications. 48

Figure A.4. DELTA PMT24V350W1AK Technical Specifications. 48

Figure A.5. ITEAD MX130731002 Step Down Converter Technical Specifications. 49

Figure A.6. Drag Coefficient table. 49

Figure Ap.1. 2D drawing of the aluminum support plates for the Power Supply and the step down converter. 50

Figure Ap.2. 2D drawing of the aluminum support plates for the Controller Board. 50

Figure Ap.3. 2D drawing of the aluminum support plates for the Cooling Fan..... 51
Figure Ap.4. 2D drawing of the axles for the wheels..... 51

LIST OF TABLES

Table 2.1. Table of dimensions. 25

Table 3.1. Values given by the software and the correspondent real values on the first tests.
..... 32

Table 3.2. Values given by the software and the correspondent real values on the second
tests..... 35

Table 3.3. Displacements for each shape suggestion. 39

Table 3.4. Masses for each shape suggestion. 40

LIST OF ACRONYMS/ ABBREVIATIONS

Acronyms/Abbreviations

ADAI – Associação para o Desenvolvimento da Aerodinâmica Industrial

LEIF – Laboratório de Estudos sobre Incêndios Florestais

SGIF – Sistema de Gestão de Informação de Incêndios Florestais

1. INTRODUCTION

According to Greek Philosophy, fire has always been a part of nature, being one of the four elements of the universe and although most often associated with the idea of destruction and catastrophe, it can also be seen as an opportunity for nature's renewal (Ferreira-Leite et al., 2013).

In Portugal, around the 1950s, the intense exodus of the rural population to both urban areas and other European countries, as a result of the socio-economic changes that took place, led to the abandonment of agricultural areas and the consequent transformation of the landscape. Traditional land use and people's lifestyles have changed profoundly and as brought an increase in large areas of abandoned farmland, many of which have become landscapes prone to high-intensity fires due to the accumulation of high levels of biomass (Ferreira-Leite et al., 2012).

Large fires then began to spread (total affected area of 100 hectares or more) and for the first time in the national statistics, in 1986 in Vila de Rei, a fire of more than 10 000 has appeared. If, until now, forest fires were not considered a key problem for the Portuguese forest, from this date a new reality began regarding large fires in Portugal (Ferreira-Leite et al., 2013) which currently represent a very serious problem, with economic, social and environmental consequences. According to (Xavier Viegas et al., 2019), forest fires are a natural and anthropogenic phenomenon that impacts the environment, the economy, causes social disruption and mobilizes most of the human and material resources allocated to Civil Protection.

Concerning the history of forest fires, the data analysis between 1990 and 2019 (figure 1.1.) shows a decreasing trend in the number of occurrences and a great variability in the annual burned area values, which presents maximum values in the years of 2003, 2005 and 2017.

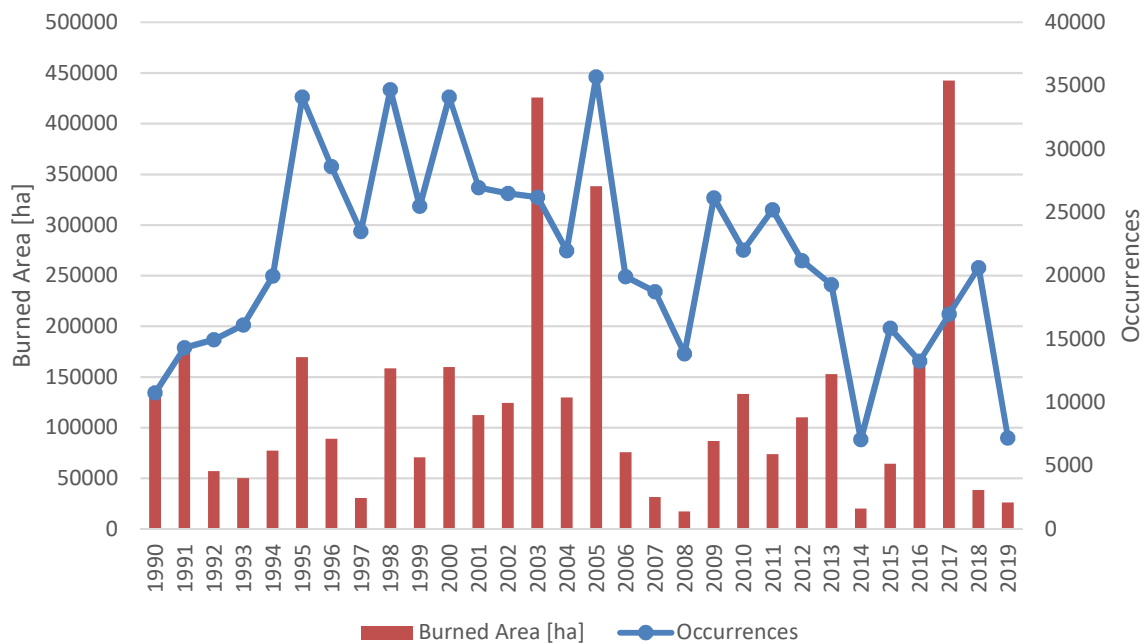


Figure 1.1. Occurrences and Burned Area in Mainland Portugal, per year, between 1990 and 2019 - Data from SGIF database.

The annual average burned area in the last three decades is 124838 hectares, while the annual average number of occurrences is 21374.

Despite the temporal irregularity in the number of occurrences and the burned area, “Continental Portugal is cyclically affected by this phenomenon, noting years, as was 2017, when the social impacts are overwhelming, both in the number of fatalities, serious and minor injuries, and environmental losses sometimes with a very long payback period (Xavier Viegas et al., 2019).

Indeed, according to data from the (10th interim report of forest fires – 2017), between January 1st and October 31st of 2017, there were a total of 16981 occurrences resulting in 442418 hectares of burned area of forest space. Of these occurrences, 214 were large fires (total affected area equal to or greater than 100 hectares) that burned 412781 hectares of forest space, about 93% of the total area burned and more than 50% of the area burned that year in Europe southern countries.

The figure 1.2. shows the distribution of burned areas in mainland Portugal as of October 31st.

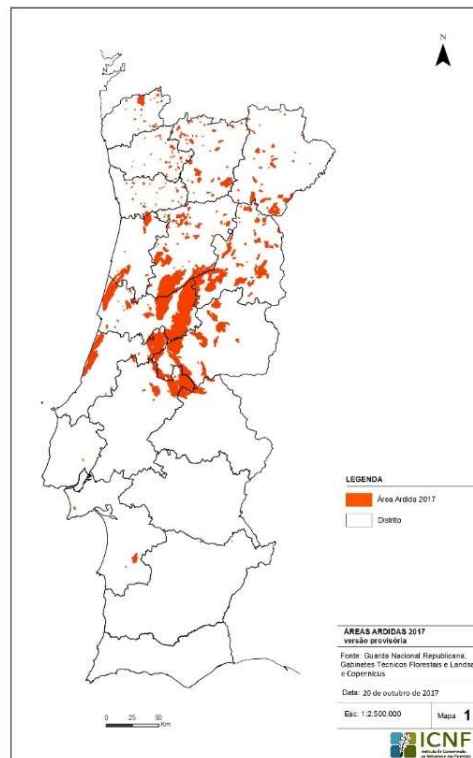


Figure 1.2. Distribution of burned areas in Mainland Portugal – October 31st – Data from the 10th interim report of forest fires – 2017

The fires of June and October of 2017 contributed decisively to these values. These fires were characterized not only by the very high area burned in a very short period of time but also by the high number of casualties among the civilian population and the high damage that affected private forest spaces, agricultural areas, national forests, business infrastructures, municipal facilities, rural tourism facilities and private housing. The extent of the fires of 2017 surpassed all previous events, even those that left a memory of enormous destruction, namely in 2003 and 2005, and created an environment characterized simultaneously by consternation, helplessness and explicit fragility of our social organization (Guerreiro et al., 2018). They also generated social debates on the subject, the creation of reports including the most varied recommendations to be taken to reverse the situation, the definition of legislative measures and the creation of awareness-raising campaigns to mobilize the population about fire prevention and firefighting and appropriate behavior and measures.

It is also in this context that scientific research has developed and produced work on fire containment and suppression mechanisms, aimed at the protection and safety of people, houses and other structures, in order to minimize the harmful impact of fires.

1.1. Motivation

The fixed thermal barriers (FTB) (figure 1.3.), consist in a system for protection against fire that uses a fireproof fabric attached to an articulated structure. The structure is then locked to a main tower, where there is a screw thread for the motors that open and close the articulated structure.

The main objective of the thermal barriers is to create safety perimeters around the area in need of protection. These areas can be houses, terrains, factories, etc. This is achieved with a hybrid system that consists of:

- The fabric, which attenuates the spread of the fire and reduces the temperature on the inside part;
- A water sprinkling system that humidifies the nearby terrain and the fabric itself.

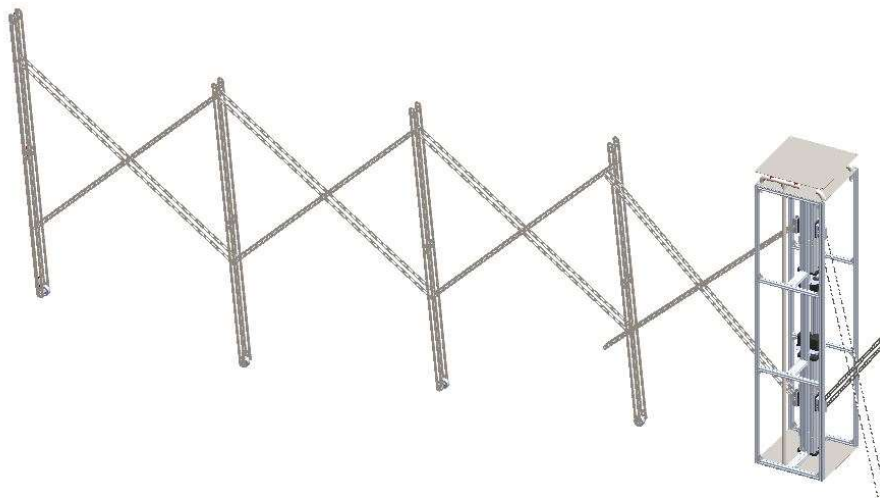


Figure 1.3. CAD design of the barrier.

This dissertation is associated with the Fireprotect project (figure 1.4.) which is coordinated by ADAI and co-financed by the European Regional Development Fund. The aim of this project is to develop, test and demonstrate several protection systems for people and elements exposed to fire. The thermal barriers, which are the main focus of this work, are one of those protection systems.



Figure 1.4. Fireprotect project logo.

1.2. Objectives

This dissertation has two main objectives. One of them is the development of a system that opens and closes the structure of the barriers and the fabric itself and the other is the implementation and optimization of the entire barrier structure. Regarding the first objective, the goal is to create a solution that allows the user to quickly activate a system that extends the structure of the barrier and the fireproof fabric attached to it.

The other objective focuses on implementing the articulated structure, attaching it to the main tower. This also includes the testing and identification of structural problems. For these, solutions are presented and the system is optimized towards greater robustness. When all the objectives are achieved, there should exist a complete structure, capable of opening and closing as the user controls it.

1.3. State of the art

As a first step to make in all research work, it is important to make a survey of existing studies and systems related to the one proposed in this work. This research focused on patents of fire protection barriers and fire protecting systems and mechanisms to apply on indoor and outdoor scenarios.

The main parameters included in this work are present on Teruel's (2009) work. This consists of a system of multilayer canvases used for controlling forest fires. These can be deployed from fixed stations or cabinets, that work as elements for storage. The deployment can be made using cables or guides with either rings or snaps. Inside the station there would be a roll with a rotating device, as can be seen on figure 1.5.

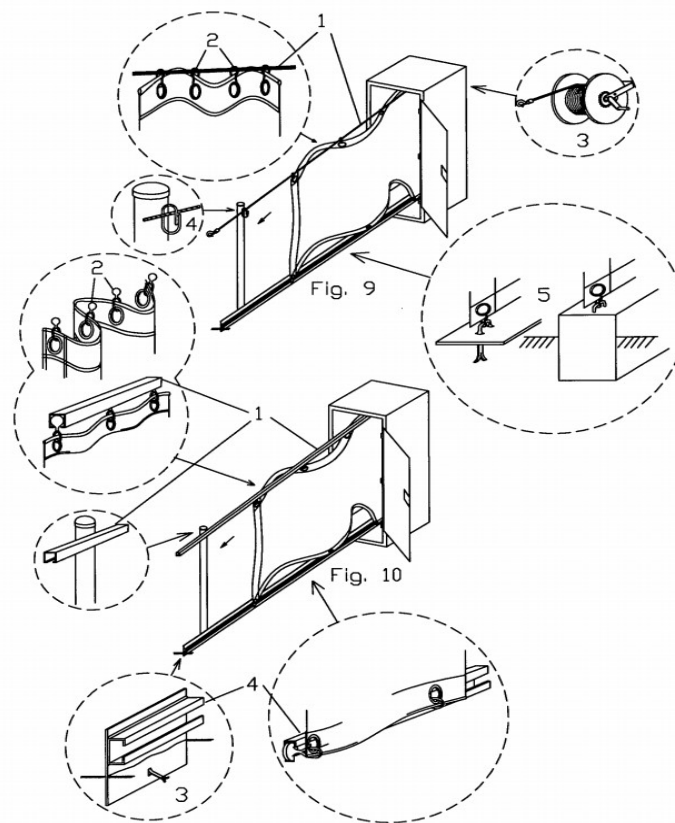


Figure 1.5. Drawings of Teruel's (2009) work.

This concept is very similar to the one proposed in this work, except in the way the canvases are deployed. It also requires some cables to be previously laid out, in which

the canvases go. Supposing the cables are stored inside the cabinet, one has to first mount the guide cables and then stretch the canvases along such cables. While the second part can be easily automated, it is difficult to automate the first part, thus this deployment solution cannot be totally automatic and autonomous, as intended for this work's proposed concept.

Linares' (2014) approach consists of a curtain composed of a fire resistant material which can be extended upwardly using hydraulic, electric or pneumatic cylinders, as seen on figure 1.6.

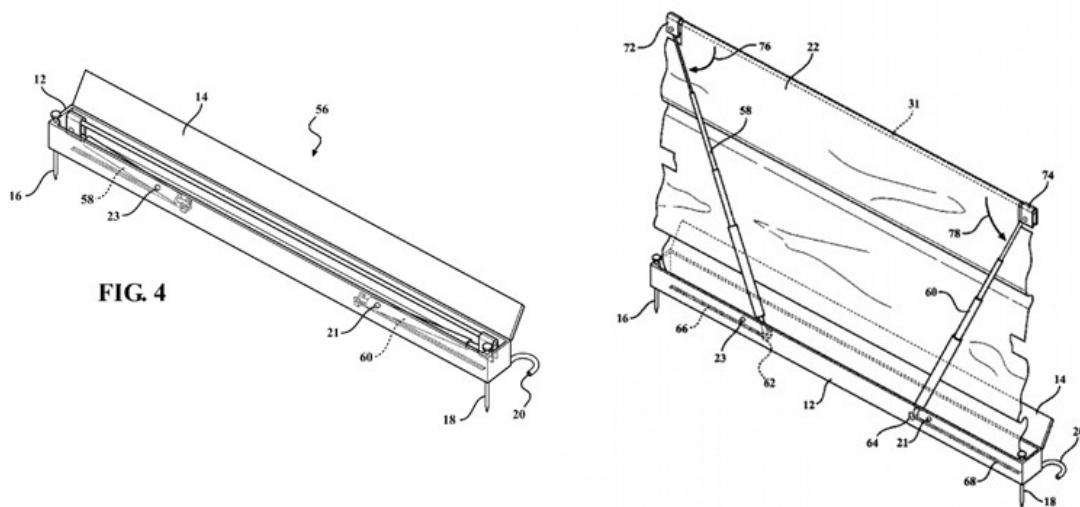


Figure 1.6. Drawings of Linares' (2014) work.

The entire structure can be stored in different housings. To respond to high speed winds, this structure has ground supported stanchions that extend to provide more fixing support.

On a different approach, an analysis was made on the work of Rogers and Holliday (2004). A wildfire protection method for houses and other structures that consists of a fireproof material that is contained on a fireproof deployment apparatus, such as rollers (figure 1.7.). This apparatus is contained and secured inside a housing that can be mounted to strategic areas. The extension of the fireproof material is made using rolls.

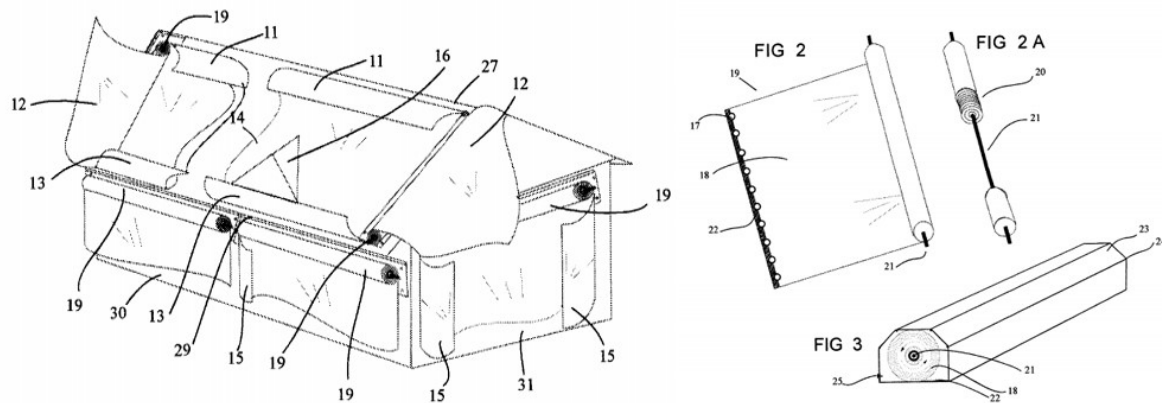


Figure 1.7. Drawings of Roger and Holliday's (2004) work.

To study different ways to extend the fabric, it was also important to analyze some indoor systems of fire protection. One of them is a solution by Coopers called FIREMASTER PLUS² FIRE CURTAIN BARRIER. It was developed to protect all building types and can be applied to protect most vertical applications. It comprises a fire resistant fabric which is wound on to a steel roller that is powered by a 24 V DC Motor. The system is enclosed inside a galvanized mild steel box and there's also a bar on the bottom edge to guarantee the deflection performance of the structure (figure 1.8.). The barriers remain invisibly retracted until activated by an alarm or detector signal and then assembly completely by gravity. While this solution is perfectly suited to protect doors or passages, as it requires a permanent frame around the curtain, it is not suitable for outdoor use due to the visual impact of such frame.

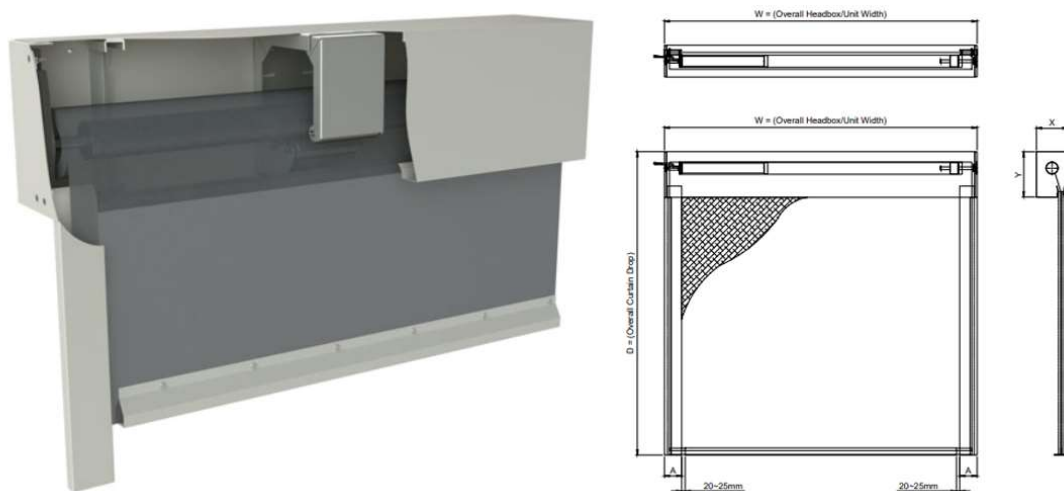


Figure 1.8. Firemaster Plus² Fire Curtain Barrier by Coopers.

The same company also has a product called FIREMASTER CONCERTINA™ “OPEN” ACTIVE FIRE CURTAIN BARRIER ASSEMBLIES. It consists of an electrically operated active fire curtain barrier assembly used to form a virtually continuous barrier as a fire separating element. It comprises a folded/pleated fire resistant fabric mounted inside a headbox and fixed to a bottom tray which is fixed either side to steel pulley tapes which are wound on to a drive shaft (figure 1.9.). The drive shaft is powered by a 24V DC electric motor. They are also enclosed within a galvanized mild steel box. When fully extended, they have a shape similar to an accordion.

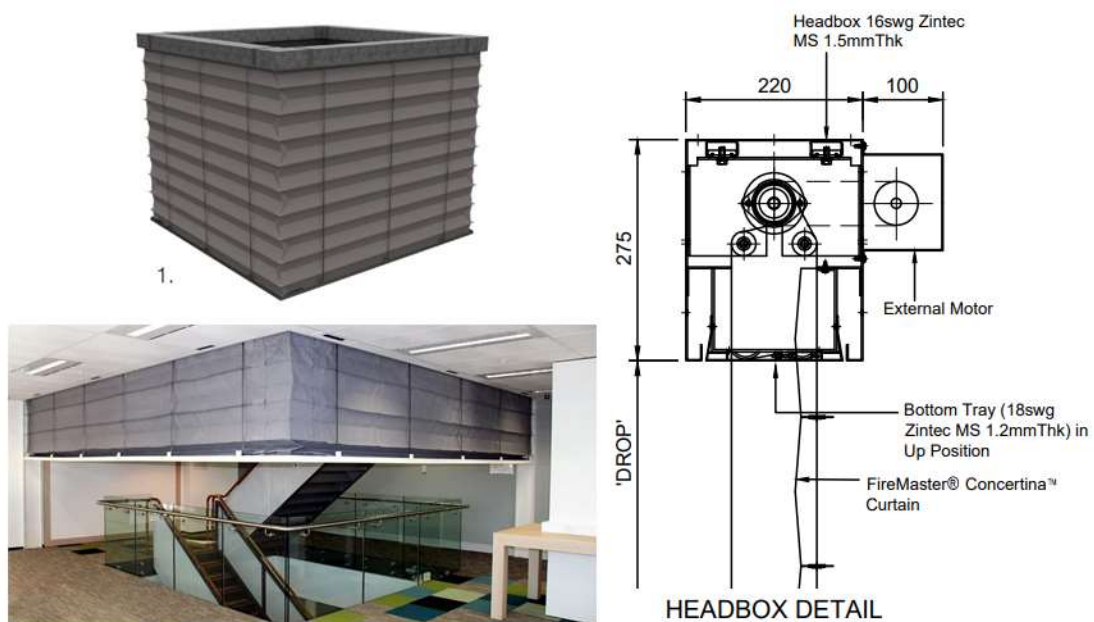


Figure 1.9. Firemaster Concertina™ “Open” Active Fire Curtain Barrier Assemblies by Coopers.

This folded fabric seems like an interesting idea to apply on this work. It allows to have the fabric in a relatively small space when the structure is closed and to extend to considerably long sizes when the structure is open. Unlike all the studied systems, in our case the fabric will be extended with an articulated structure. The opening and closing of the structure will use a mechanism similar to the ones used on the Coopers systems, with a system of motors and actuators controlled by the user.

2. METHODOLOGY

2.1. Hardware

2.1.1. Controller Board

To open and close the structure, a pair of motors was used. In order to drive the motors and the actuators, there was a need to use some type of hardware. The chosen system was a Duet 2 Wifi controller board, by Duet3D (figure 2.1.). These boards use a wireless connection to operate and can be controlled with a computer or a smartphone, since it only requires an wi-fi connection and a browser to work.

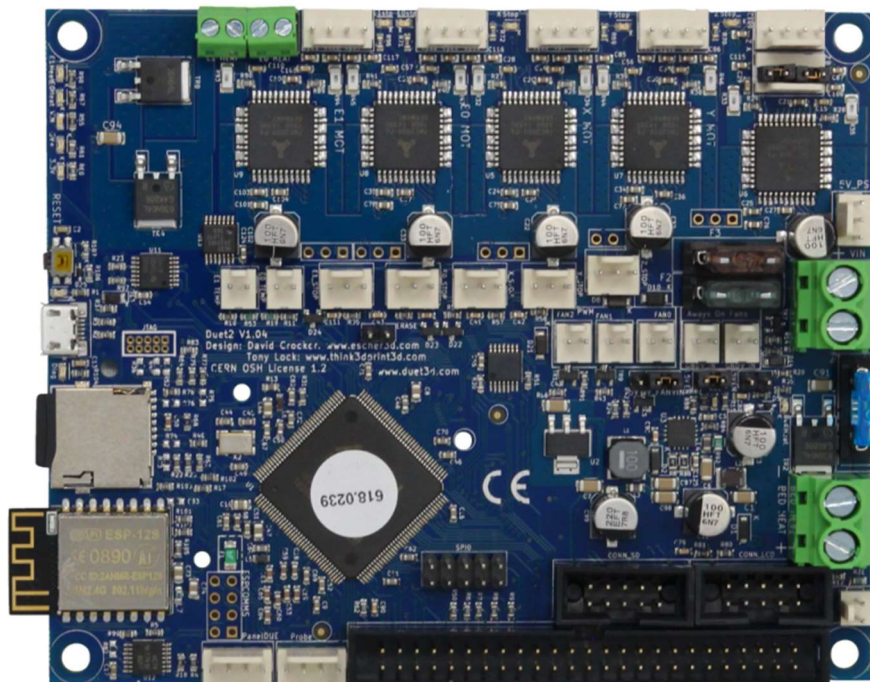


Figure 2.1. Duet 2 Wifi.

2.1.2. Actuators

The actuators used were the C-Beam XLarge Linear Actuators, together with the high-torque Nema 23 Stepper motor by Openbuilds (figure 2.2.).



Figure 2.2. C-Beam XL Nema 23 Actuator.

2.1.3. Cooling Fan

With the operation of the motors, the temperature of the Controller Board's drivers tends to increase. To avoid overheating and damaging the board, a cooling fan was used to decrease the temperature and assure the correct operation of the system (figure 2.3.). The fan used was the COOLER MASTER - Sickle Flow 120mm Blue LED Fan 2000rpm 69 69 CFM Long-Life Sleeve 50.000H.

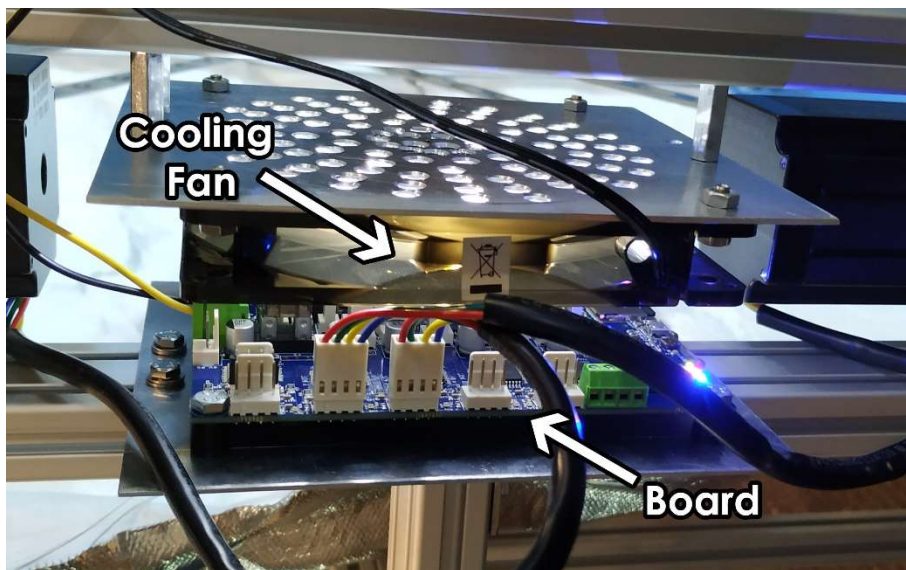


Figure 2.3. Controller board with the fan.

2.1.4. Power Supply

To power the controller board, a power supply was used (figure 2.4.). It needed to have an output voltage of 24V and a power of 350W, which were the requirements for the board. The model used is the DELTA PMT24V350W1AK.



Figure 2.4. Power Supply.

However, the cooling fan used had an input voltage of 12V, which is inferior to the output voltage of the power supply, that works at a voltage of 24V.

Thus, there was a need to use a Step Down Converter, that converts voltages from 24V to 12V, with an electric current of 2A (figure 2.5.). The model used was the ITEAD MX130731002 - LM2596 DC-DC Buck Converter Step-Down Power. The cables coming from the power supply and going to the cooling fan were all welded to the Step Down Converter. Since it has variable outputs, it was necessary to adjust it to our needs, using a multimeter. It allowed to configure the output value of the Step Down to 12V by adjusting the high precision potentiometer embedded in the board. With this addition it was possible to use the controller board and the cooling fan with a single power supply.

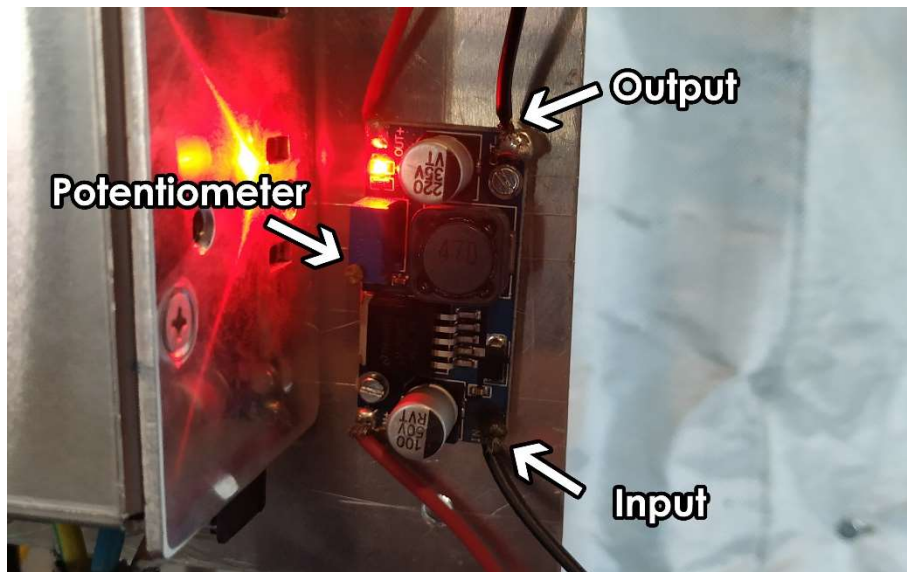


Figure 2.5. Step Down Converter.

All of these components were attached to the main tower using aluminum support plates that were cut with the dimensions of the parts and fixing holes and then bolted to the structure.

2.2. Software

2.2.1. User interface and communication

The first step was to configure a Wi-Fi connection to control the board. For this, the board was connected to a computer via USB and using the YAT software, a network was configured, introducing the SSID and the password.

The Wi-Fi network used was from a hotspot created by the mobile data of a smartphone. This type of configuration can be an interesting alternative, since it is always available, avoiding the need of a fixed Wi-Fi network.

At the end of the configuration, the software returns an IP address, which can be used on any Internet browser. This address allows the user to have access to the controller board's software (figure 2.6.).

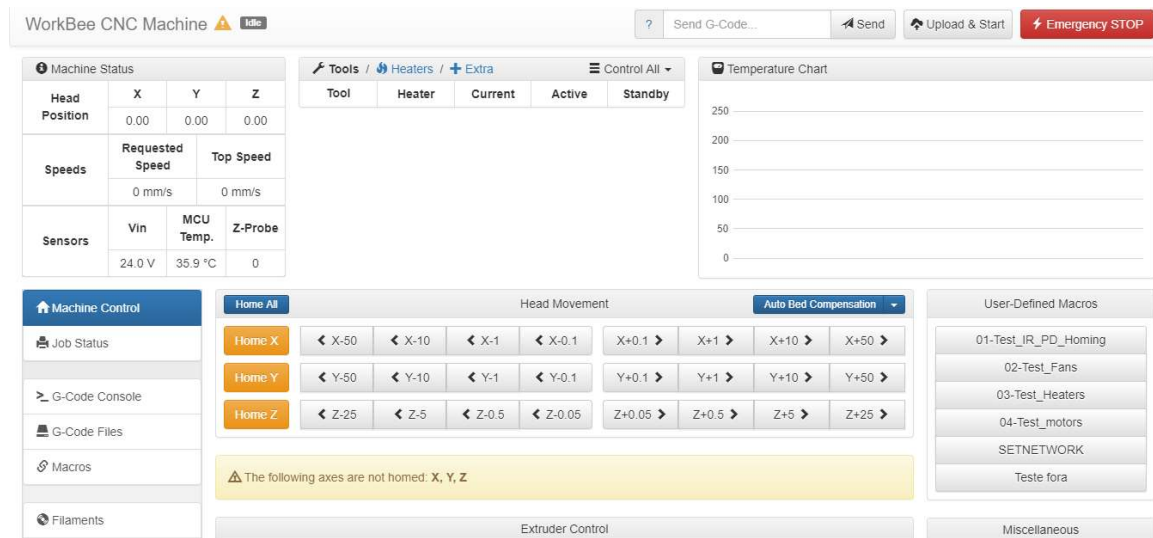


Figure 2.6. Print Screen of the software.

Finally, one of the motors from the structure was connected to the stepper motor X and the other one to the stepper motor Y.

2.2.2. Programming

The controller board's software uses a type of code called G-Code. This is a very common code type, used frequently to control CNC machines. In this case the code has the following structure:

G91 G1 Ya Xb Fc

Figure 2.7. Generic G-Code Example.

The “G91” and the “G1” parts of the code remained intact for all the codes used, since the “G91” part represents the relative position of the motors and the “G1” represents the instruction to move the motors.

The “Y” and “X” represent the stepper motors connected, that in this case were only X and Y. The “F” represents the speed in which the motors will rotate. The “a” and “b” values are the movement in each axis, in millimeters. The “c” value represents the value of the rotating speed, in millimeters per minute.

Here's an example of a code used in this work:

G91 G1 Y-400 X400 F5000

Figure 2.8. Example of a G-Code.

In this example, the motor Y will move 400 mm in one direction and the motor X will move 400 mm in the opposite direction, at a rotating speed of 5000 mm/min.

In order to perform the process of extending the barrier, and due to the wiring connection of the actuators, which in turn defines the positive direction of the axis of movement (figure 2.5.), the motors must rotate equal measures in opposite directions, meaning that the values associated with X and Y were always additive inverses (figure 2.9.).

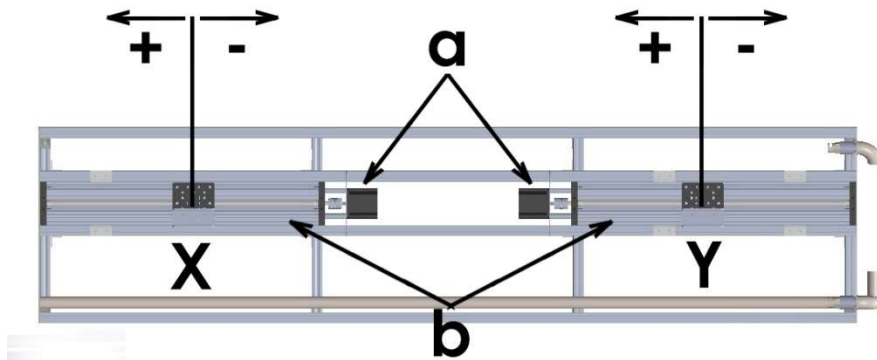


Figure 2.9. Scheme of the directions of the motors. The letter a represents the motors and the letter b represents the actuators.

2.3. Structure Implementation

The first step of the implementation was to make a verification of the parts previously acquired and, considering the 3D models of the structure and the work of Costa (2018) acquire the remaining material for the full assembly.

Besides that, it was also needed to order some custom-made parts. One of them was a spacer to put between two X bars (figure 2.10.).

These, together with the use of washers, allowed us to keep a constant distance between the articulated bars.



Figure 2.10. Spacer separating the bars.

Afterwards, the axles for the wheels were created from a bar with a diameter of 8 mm, that was cut in bars with a length of 40 mm and then machined on both ends so that they would have a diameter of 7 mm (figure 2.11.). This was the diameter of the hole on the ball bearings used.



Figure 2.11. Axle for the wheels.

The first time the structure was implemented, with the intention of testing, the assembly was made only with two vertical supports, one intermediate and one final (figure 2.12.). Because of that we only needed to use two wheels and, consequently, two axles.



Figure 2.12. First assembly of the structure.

The structure was projected to have two of the narrower vertical bars (figure 2.13.) parallel to each other in each of the intermediate vertical supports and two of the wider vertical bars (figure 2.14.) in each of the final vertical supports, also parallel.



Figure 2.13. Narrower vertical bar.

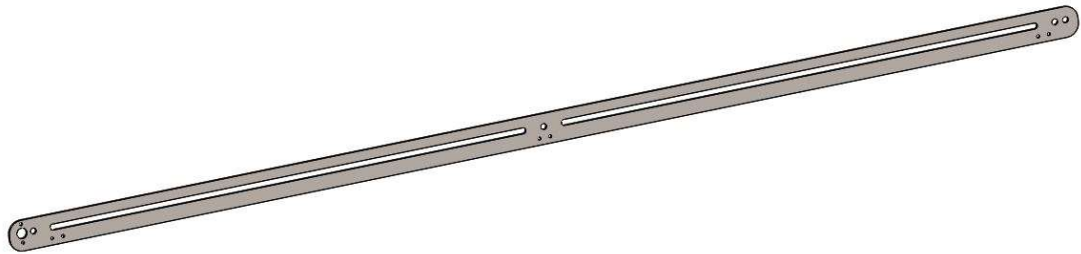


Figure 2.14. Wider vertical bar.

When the assembly of the barrier was concluded, it was noted that it had stability problems. When it was fully extended, the structure could balance back and forth, due to lack of support, thus rendering it useless in a real case scenario. Because of that, it was necessary to make a new approach to the construction of the barrier and create a new solution.

This solution consisted in the alteration of the vertical supports' format, allowing it to have more stability. For that, the wider vertical bars, that initially were intended to be used on the vertical support of the far end of the structure, were now used on both vertical supports as a pair and the wheel between them was removed. A pair of the narrower vertical bars was then attached to each side of the wider bars.

Finally, a wheel was put between both vertical narrower bars. The detail gets clearer on the following figures:

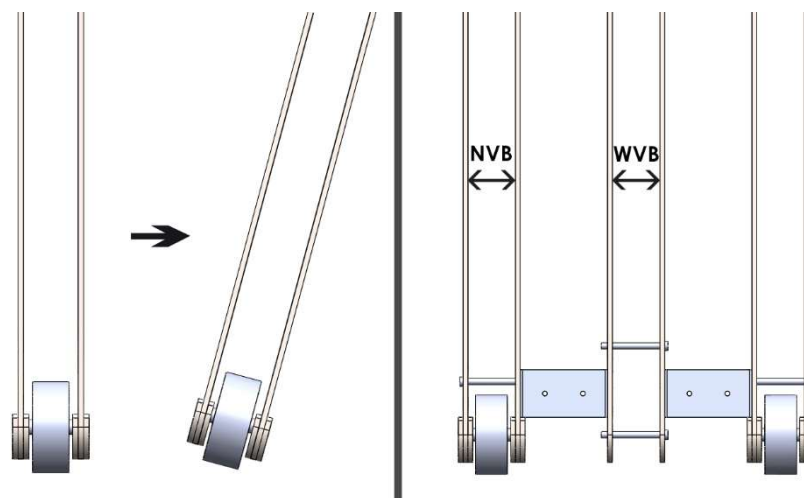


Figure 2.15. Old approach (on the left) and new approach (on the right).



Figure 2.16. Detail of the new approach of the vertical supports.

On the spaces between the pair of narrower bars and the pair of wider bars three pieces were put to assure stability and preventing them to shake (figures 2.17. and 2.18.). They also allowed to keep a constant distance between bars.



Figure 2.17. Pieces used to space bars.

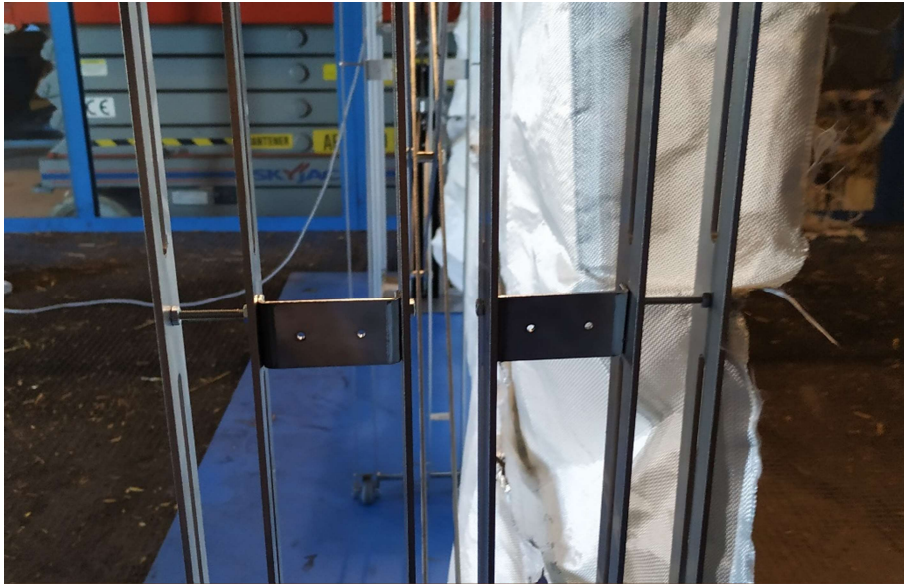


Figure 2.18. Pieces applied on the structure.

To assure resistance and stability to the pair of bars, a combination of nuts and bolts was used. It also allowed to keep a constant distance of 30 mm between the pair of narrower bars and the pair of wider bars, which was also the dimension of the thicker part of the axles.

When the structural assembly was concluded, it was noted that the X bars (figure 2.19.) were not as stiff as the rest of the structure and bent very easily. This caused the articulated structure to remain unstable when subject to large forces and even during opening and closing. To solve this, a new approach using different shapes for the X bars was proposed. To find the most suitable shape, several simulation tests were performed. This optimization problem is the subject of the next chapter.



Figure 2.19. X bars.

The final step was the attaching of the flameproof fabric to the structure. The fabric was cut in two stripes, which were then connected to each other, forming a section of 233 x 150 cm (figure 2.20.).



Figure 2.20. Fabric cut.

It was then folded in an accordion shape so that the structure would have a smoother opening and closing, preventing the fabric to fold in less convenient places. After this, it was attached to the structure, using the bolts previously used to assure distance between bars. This concluded the implementation of the full structure.



Figure 2.21. Final extended structure.



Figure 2.22. Closed structure.

2.3.1. Airflow Resistance

It was then important to calculate the width that the structure should have, depending on the wind speed. To make these calculations, the following schemes were used:

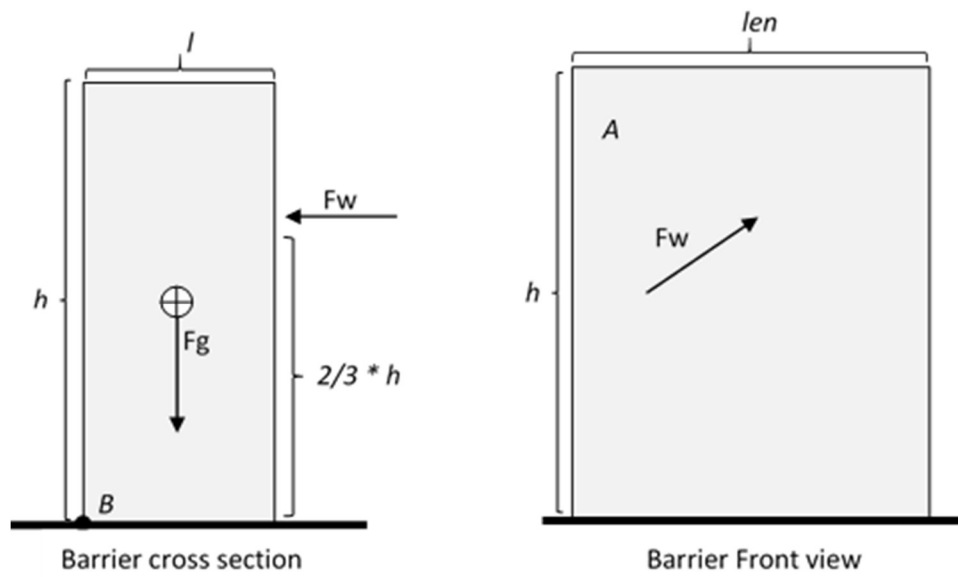


Figure 2.23. Schemes used for the calculations.

Some assumptions were made:

- No boundary layer (uniform wind profile);
- Wind force applied at 2/3 of total height;
- Structure not fixed to ground.

The following table groups the values used for every term of the equations:

Table 2.1. Table of dimensions.

Dimension	Meaning	Value	Unit
h	Height of structure	1,5	m
l	Width of structure	Variable	m
F_g	Weight of structure	200	N
F_w	Wind Force	Variable	N
M_g	Weight momentum	Variable	N.m
M_w	Wind momentum	Variable	N.m
len	Barrier length	2,33	m
ρ	Air density (@1 atm and 15°C)	1,225	Kg.m ⁻³
C_D	Drag coefficient (Narrow strip, face on)	1,98	

Equilibrium state:

$$M_g - M_w = 0 \quad (2.1)$$

Applying momentum expressions, relative to point B:

$$F_g \frac{l}{2} = F_w \frac{2h}{3} \quad (2.2)$$

The wind force is given by:

$$F_w = C_D * A * P \quad (2.3)$$

Where C_D is the shape drag coefficient, A is the surface area, given by $len * h$, and P is the wind Pressure with the assumptions considered previously, and given by:

$$P = \frac{1}{2} \rho U^2 \quad (2.4)$$

Where U is the wind speed. Thus, by combining the equations we obtain:

$$F_g * \frac{l}{2} = C_D * len * h * \frac{1}{2} \rho * U^2 * \frac{2h}{3} \quad (2.5)$$

Solving structure length in terms of wind speed:

$$l = \frac{2 * C_D * h^2 * len * \rho * U^2}{3 * F_g} \quad (2.6)$$

The graphic of figure 2.24 represents the values of structure width as a function of wind speed for the new approach of the vertical support bars, considering a weight force of 200 N:

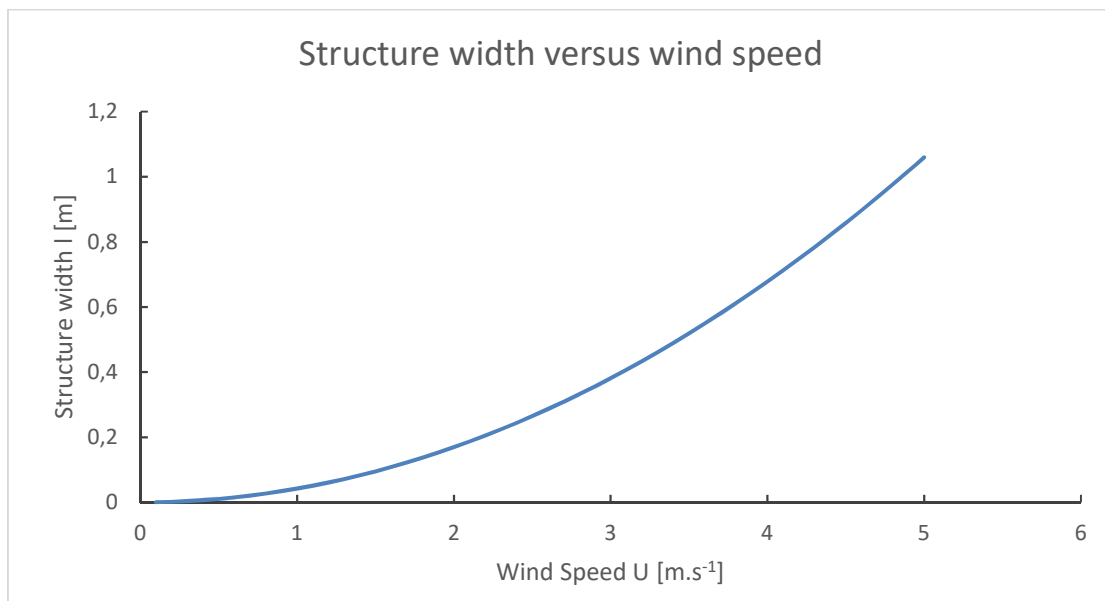


Figure 2.24. Structure width versus wind speed (new approach).

The graphic of figure 2.25 represents the same values but for the old approach of the vertical support bars, considering a weight force of 90 N:

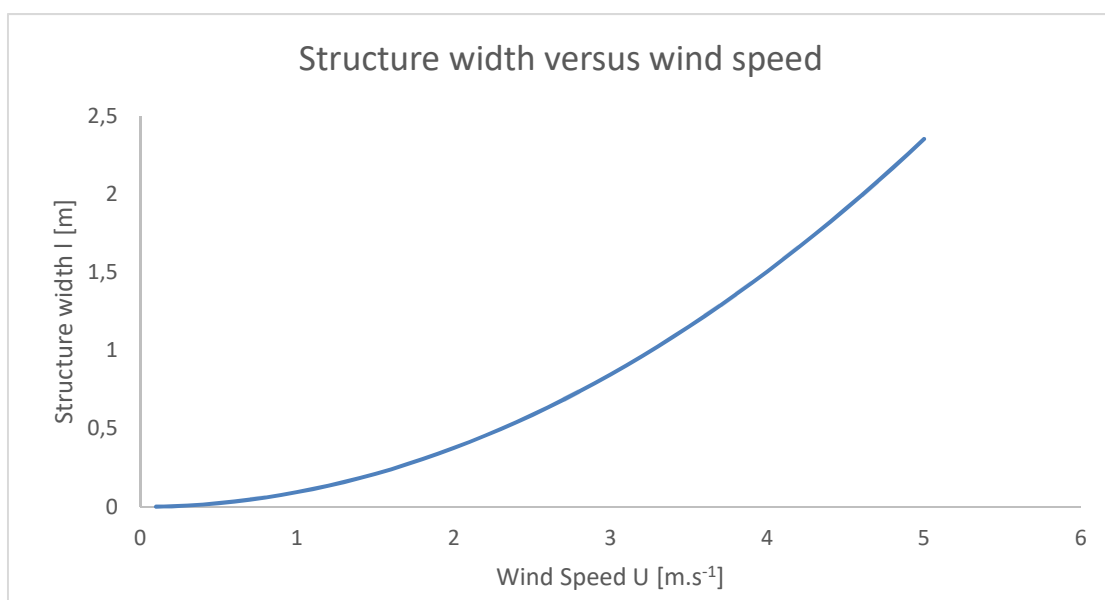


Figure 2.25. Structure width versus wind speed (old approach).

These calculations were made for a non-fixed structure, unlike our case, in which the structure is fixed on both ends. Because of this it doesn't require a width as great as in this case to support wind. The fixation on both ends effect was not included because there is no clear idea of the fixation force. This force depends on the type of fixation (screwed, with concrete, etc.) and on the type of soil (sandy, rocky, etc.), so it is very variable. Besides this, the purpose of these calculations was to see which would be the needed width for the structure to remain standing without being fixed on the soil, just to have an idea of the impact that the variation of the width has on the stability of the structure.

:

3. TESTS

3.1. Laboratory Tests

3.1.1. Methodology

The main objective of the laboratory tests was to analyze the resistance of the structure when subjected to an air flow, which simulates the wind conditions expected in an outdoor environment. For that, the structure was assembled on the wind tunnel in LEIF, fully extended (figure 3.1.), and put to test with different values of air flow velocity.



Figure 3.1. Fully extended structure on the wind tunnel.

Two cameras were used: one on each side of the structure. The first camera (Camera 1) was put at the same level as the barrier and the second one (Camera 2) was put on the top of a platform elevator (figure 3.2.).



Figure 3.2. Positions of the cameras.

The cameras were used to film the behaviour of the structure at different air flow velocities. The frames of the videos were analyzed and used to evaluate how much the structure moved for each air flow velocity. The most important frames will be the ones that show the biggest movement for each air flow velocity.

Two slightly different types of tests were done. On the first tests, the structure was put on the wind tunnel and it was subjected to air flow velocities of 1, 2, 3 and 4 m/s. The movement of the structure was analyzed on the vertical support of the far end, in this case, using the images from Camera 1.

The structure is designed to have another similar structure attached to it on the far end. To simulate this, on the second tests, the far end was fixed, so that the movement was analyzed on the middle vertical support, using the images from Camera 2.

3.1.2. Results

3.1.2.1. First Tests

To make the calculations and the interpretation easier, a line was drawn on the images representing the width of the structure and a different color was used for each air flow velocity: Red for 1 m/s, green for 2 m/s, yellow for 3 m/s and purple for 4 m/s.

Because the width of the structure is known to be 225 mm, there is only the need to compare the distances between each line and create a scale. This way we were able to determine how much the structure moved with each air flow velocity.

When the air flow velocity was 1 m/s the structure didn't move. On the image below, the blue line represents the initial position.



Figure 3.3. Initial position of the structure.

On the following image there is a representation of the line for each of the air flow velocities:

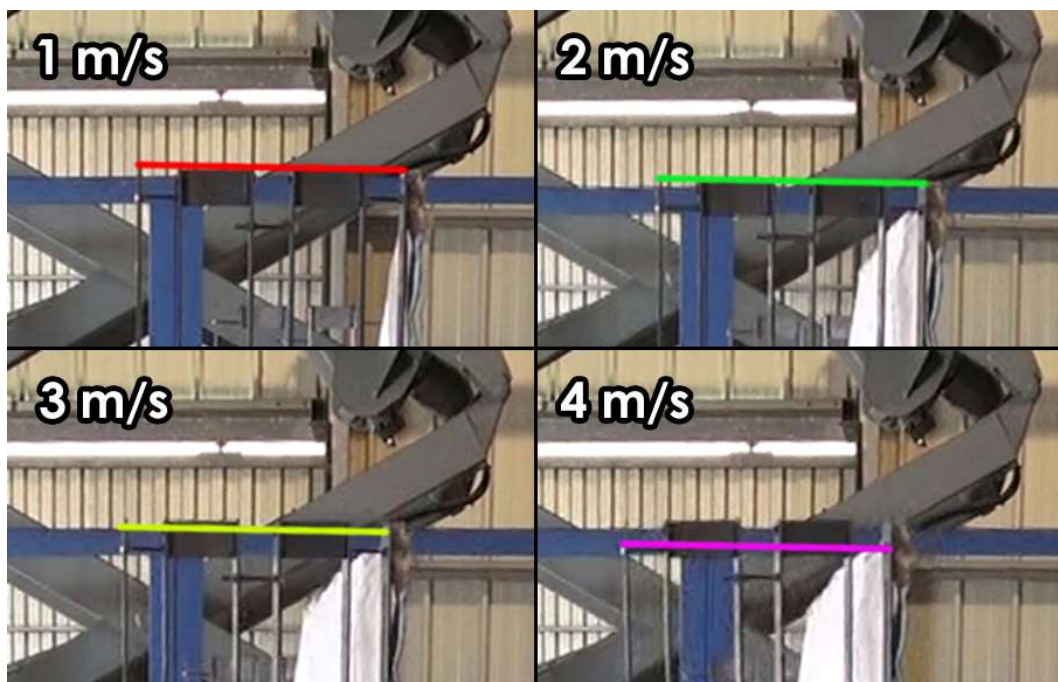


Figure 3.4. Representation for every air flow velocity.

We were now able to separate all the lines and analyze them to get the correct values for the movement of the structure.

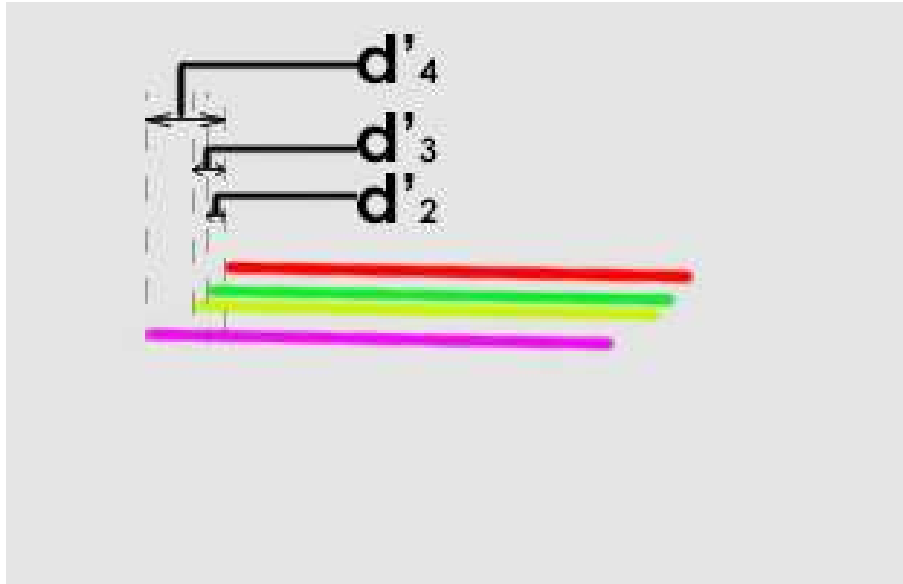


Figure 3.5. Lines representing all the positions of the structure.

To obtain the distances between the tips of the lines on the images, the software Adobe Photoshop was used. The software gives a value for the dimension of the lines that will be converted to real dimensions. The width of the structure, 225 mm, corresponds to a distance of 1,37 on the image, using a zoom of 300%. We are now able to calculate the movement of the structure using the following formula:

$$d[\text{mm}] = \frac{225[\text{mm}] * d'_{speed}}{1,37} \quad (3.1)$$

The next table groups the values obtained with the analysis of the images and the converted values:

Table 3.1. Values given by the software and the correspondent real values on the first tests.

d'_1	d_1 [mm]	d'_2	d_2 [mm]	d'_3	d_3 [mm]	d'_4	d_4 [mm]
0	0	0,06	9,854	0,1	16,423	0,24	40,299

3.1.2.2. Second Tests

The procedure was very similar to the first tests, but in this case the width of the structure, 225 mm, corresponded to a distance of 3,39 on the image, using a zoom of 100%.

Again, when the air flow velocity was 1 m/s the structure didn't move. On the image below, the orange line represents the initial position.

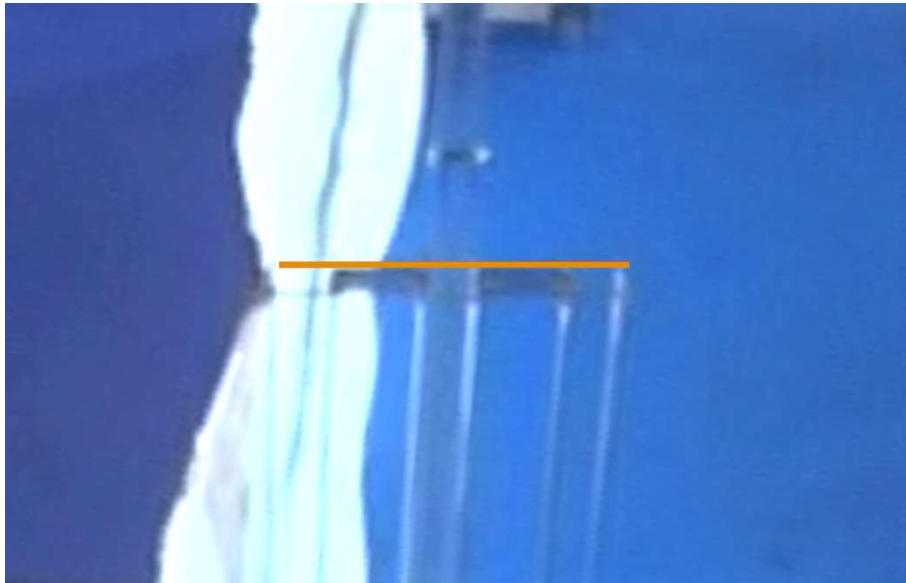


Figure 3.6. Initial position of the structure.

On the following image there is a representation of the line for each of the air flow velocities:

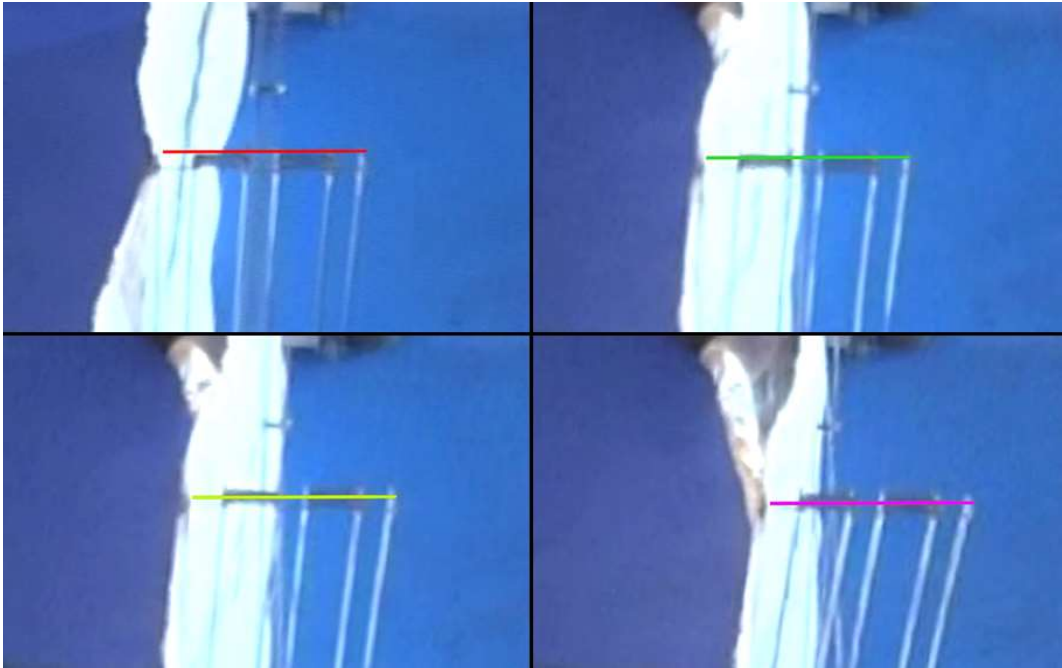


Figure 3.7. Representation for every air flow velocity.

Again, all the lines were separated and analyzed to get the correct values for the movement of the structure.

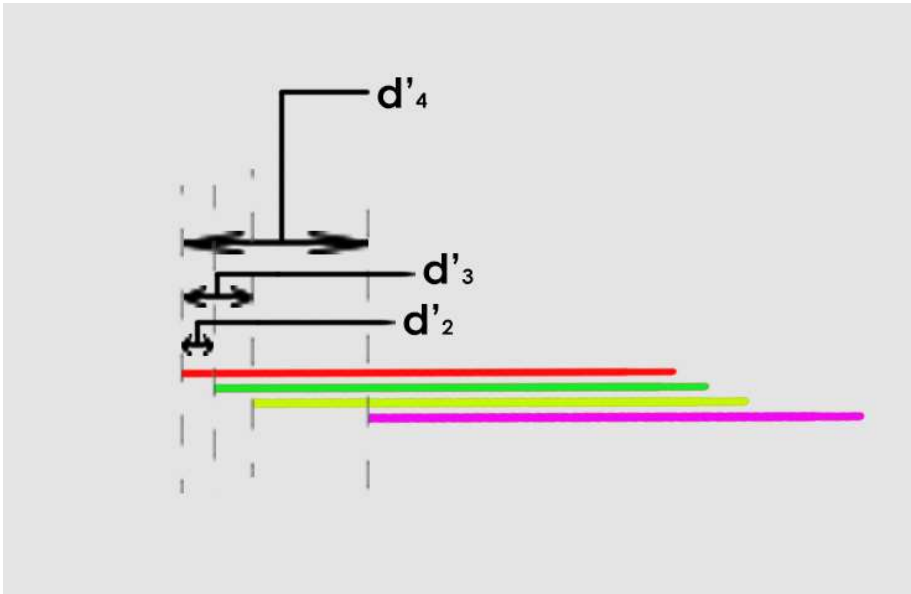


Figure 3.8. Lines representing all the positions of the structure.

Due to the different value given by the software, the new formula is:

$$d[\text{mm}] = \frac{225[\text{mm}] * d'_{\text{speed}}}{3,39} \quad (3.1)$$

Table 3.2. Values given by the software and the correspondent real values on the second tests.

d'_1	d_1 [mm]	d'_2	d_2 [mm]	d'_3	d_3 [mm]	d'_4	d_4 [mm]
0	0	0,23	15,265	0,49	32,52	1,28	84,956

3.1.3. Discussion

For both tests, all the converted values were represented on a graphic as a function of air flow velocity:

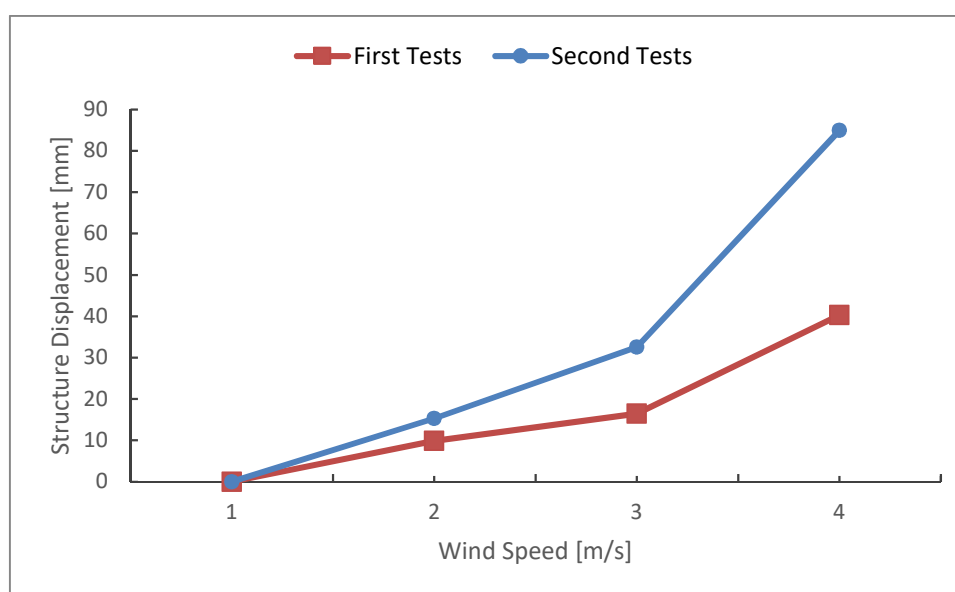


Figure 3.9. Structure displacement as a function of air flow velocity.

On the first tests, in which the structure wasn't secured on the far end, the movement was inferior than on the second tests, when the structure was locked on both ends. The far end had a maximum movement of 40,299 mm at a speed of 4 m/s while the middle vertical support had a movement of 84,956 mm at the same wind speed. This can be explained by the difference in both setups. In the second tests, due to the articulated structure being fixed on both ends, it was capable of coping with a larger displacement, when compared to the first tests, where the structure was only fixed on one end.

3.2. Simulation Tests

3.2.1. Methodology

As beforehand mentioned, the X bars had bending and stability issues that resulted in problems when closing the structure. Those could be caused by the long and thin bars, or by the type of material, which was stainless steel AISI 304. To verify this, some simulation tests were run using the Solidworks SimulationXpress Analysis Wizard tool.

On the simulation tests, the material of the bars was kept, and the only modification made was the shape. There were two new suggestions, both with the same length as the initial articulated bars: A circular section bar with an external diameter of 20 mm and a thickness of 2 mm, and a bar with square section and a thickness of 2 mm.

To perform the tests, it was necessary to define some parameters. The first of them was where to apply the fixture, which was the surface that should be kept fixed. Regarding the articulated bars, the surface used was the hole on the bottom. On the circular section bar and on the square section bar, the chosen surface was the bottom one. Then, it was necessary to define a value and a surface to apply the load. A compression load of 10 N was used on the far end for all the parts.

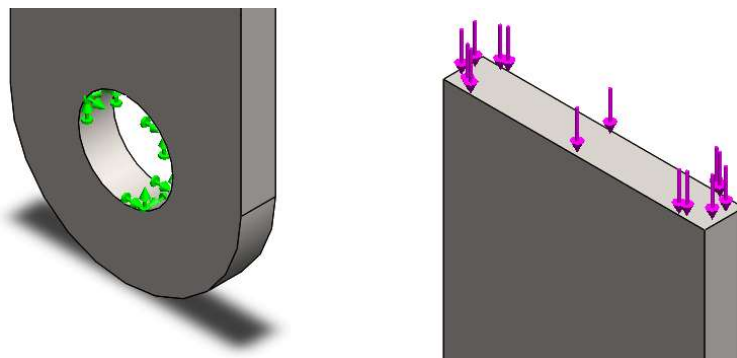


Figure 3.10. Fixtures (on the left) and loads (on the right) applied on an articulated bar.

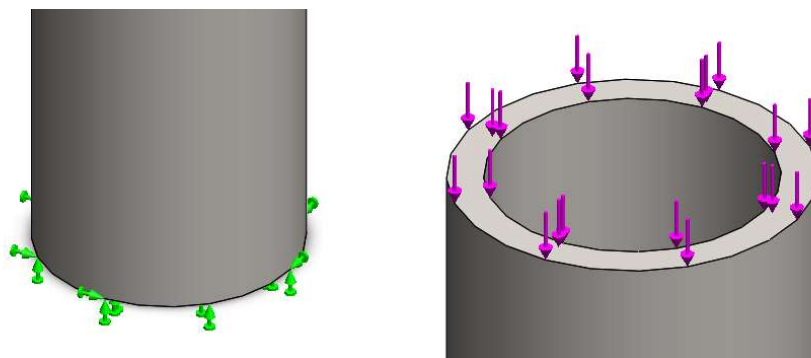


Figure 3.11. Fixtures (on the left) and loads (on the right) applied on a bar with circular section.

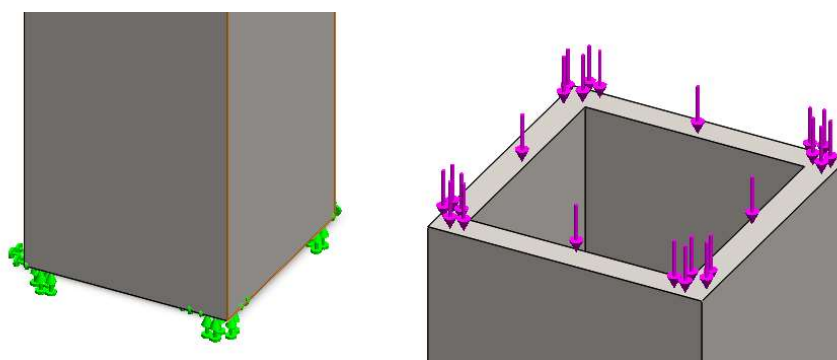


Figure 3.12. Fixtures (on the left) and loads (on the right) applied on a bar with square section.

At the end of these simulation tests, the software calculates the displacements that happen on the bar when subjected to the load previously described, which are going to be compared and analyzed afterwards.

Another important value that the software calculates is the mass of each suggestion, that will then be compared.

3.2.2. Results

The software calculated the displacements for every geometry of the bars. For the articulated bar:

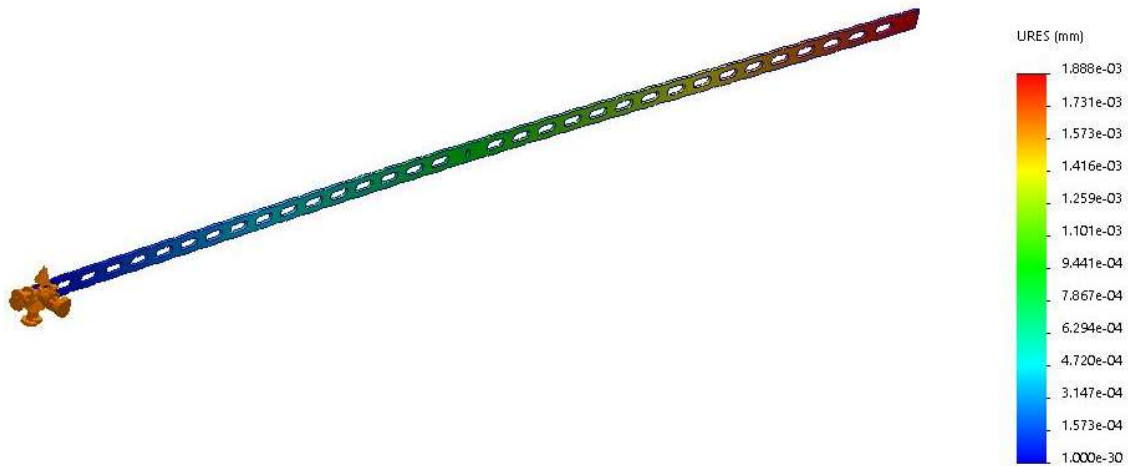


Figure 3.13. Displacements of the articulated bar.

In this case, the maximum displacement was $1,888 \times 10^{-3}$ mm.

For the circular section bar:

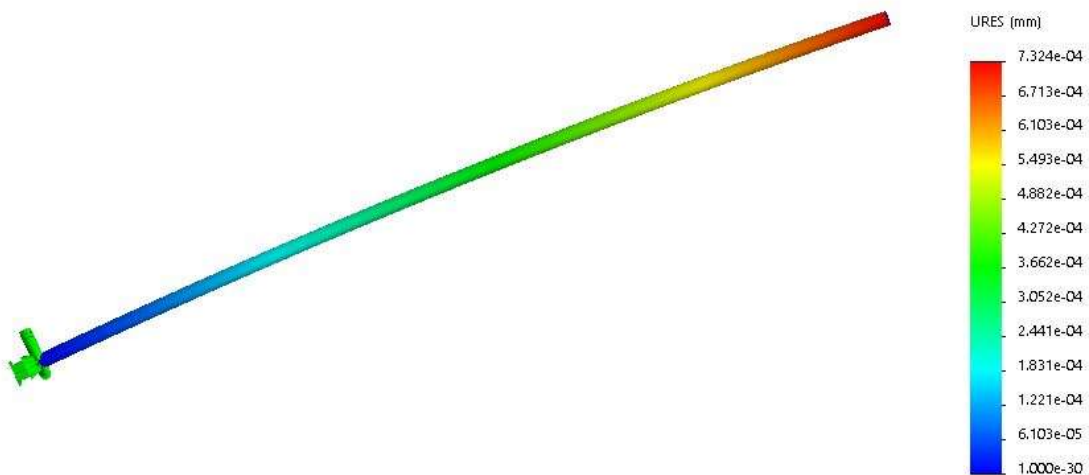


Figure 3.14. Displacements of the circular section bar.

In this case, the maximum displacement was $7,324 \times 10^{-4}$ mm.

For the square section bar:

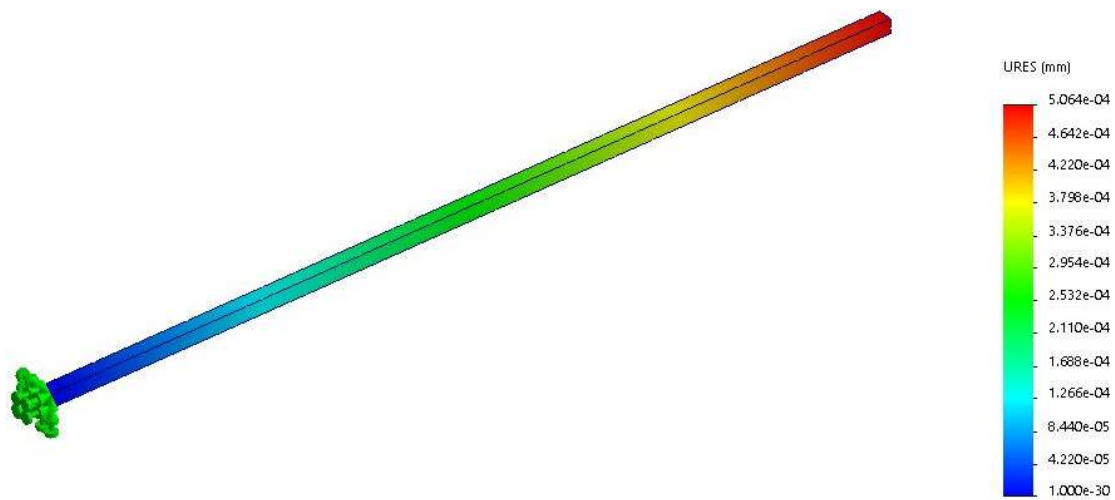


Figure 3.15. Displacements of the square section bar.

In this case, the maximum displacement was $5,064 \times 10^{-4}$ mm.

3.2.3. Discussion

The results for the maximum displacement for each result were grouped on table

3.3.:

Table 3.3. Displacements for each shape suggestion.

DISPLACEMENTS	
Articulated bar	1,888E-3 [mm]
Circular section	7,324E-4 [mm]
Square Section	5,064E-4 [mm]

Both the circular section bar and the square section bar had a smaller displacement than the articulated bar.

The masses of each suggestion were grouped on table 3.4.:

Table 3.4. Masses for each shape suggestion.

MASSES	
Articulated bar	0,50023 [kg]
Circular section	1,25402 [kg]
Square Section	1,59667 [kg]

As expected, the square section bar is the one with the biggest mass value, followed by the circular section bar.

Both new suggested solutions have bigger mass and smaller displacements than the articulated bars when subjected to the same compression load. This could make them viable since, they would bend less than the present solution and the increase of mass can make them more stable.

4. CONCLUSIONS

4.1. Achievements

At the end of this work some conclusions can be drawn. Both objectives set at the beginning of this dissertation were achieved with success.

The system to extend the fabric and the articulated structure is a viable solution that works very well and is easy for the user to control it with a distance, requiring only a smartphone with a mobile connection to the Internet.

The starting point of this work was a design which presented some flaws. These flaws were identified during implementation, the problems were addressed from a theoretical and practical point of view and some improvements were made.

The articulated structure, with its new approach is now much more stable and sturdy. The laboratory tests, especially the second tests, showed that the structure can withstand wind speeds up to 4 m/s. Regarding this, it is important to conclude that the results of the second tests are the ones that should be more taken into account, since these tests were closer to the real application of the barriers, with the articulated structure being fixed on both ends.

This solution is novel in both market and literature and is the subject of a paper which is being prepared, containing the development work done within this thesis..

4.2. Future Work

After all the conclusions were drawn, there is still room for improvement on future works.

Regarding the construction of the barriers it is important to find a solution to replace the X bars, since they seem to be the weakest link of the structure. This can be done by either adopting a new shape which ensures a smaller displacement under load, as

proposed in the previous chapter, or using stiffer materials such as carbon fiber, which may allow to maintain the low mass, while increasing the stiffness.

There is also the need to make the implementation of the water systems, with the sprinklers and water circuit. The placement of the sprinklers should be studied in order to optimize their performance in both projecting water to the ground and also to the fabric, to act as cooling mechanism.

The final development step is to test the entire solution with fire, first inside the laboratory and then in large scale field experiments

BIBLIOGRAPHY

- Comissão Técnica Independente, Guerreiro J., Fonseca C., Salgueiro A., Fernandes P., Lopez Iglésias E., de Neufville R., Mateus F., Castellnou Ribau M., Sande Silva J., Moura J. M., Castro Rego F. e Caldeira D. N. - Coords. (2018). Avaliação dos incêndios ocorridos entre 14 e 16 de outubro de 2017 em Portugal Continental. Relatório Final. Comissão Técnica Independente. Assembleia da República. Lisboa. 274 pp.
- COOPERS, SPECIFICATION FIREMASTER® A1 CONCERTINA™ “OPEN” ACTIVE FIRE CURTAIN BARRIER ASSEMBLIES: https://www.coopersfire.com/system/files/private/Coopers_Specification_FireMaster_Concertina_Open_BS8524.pdf
- COOPERS, SPECIFICATION FIREMASTER® PLUS2 ACTIVE FIRE CURTAIN BARRIER ASSEMBLIES: https://www.coopersfire.com/system/files/private/Coopers_Specification_FireMaster_Plus2_BS8524.pdf.
- Costa, M., (2018), “Structural design and analysis of an active forest fire propagation barrier”, Dissertação de Mestrado em Engenharia Mecânica na especialidade de Energia e Ambiente, Departamento de Engenharia Mecânica, Faculdade de Ciências e Tecnologia, Universidade de Coimbra, Coimbra.
- Departamento de Gestão de Áreas Públicas e de Proteção Floresta. (2017), “10.º Relatório provisório de incêndios florestais”, Instituto da Conservação da Natureza e das Florestas: <http://www2.icnf.pt/portal/florestas/dfci/Resource/doc/rel/2017/10-rel-prov-1jan-31out-2017.pdf>.
- Ferreira-Leite, F., Bento-Gonçalves, A., Lourenço, L. (2012), “Grandes Incêndios Florestais em Portugal Continental. Da história recente à atualidade”, Cadernos de Geografia, Faculdade de Letras da Universidade de Coimbra, Departamento de Geografia. Nº 30/31. pp. 81-86.
- Ferreira-Leite, F., Bento-Gonçalves, A., Lourenço, L., Úbeda, X. e Vieira, A. (2013), “Grandes Incêndios Florestais em Portugal Continental como Resultado das Perturbações nos Regimes de Fogo no Mundo Mediterrâneo”, Silva Lusitana. Nº Especial 1-9. pp. 131.
- Linares, M.A. (2014), “Extensible And Ground Support Fire Curtain”
- Ortiz Teruel, V. (2009), “Multilayer Fire-Barrier Canvases”
- Rogers, W., Holliday C. (2004), “Fire Protection Cover Apparatus For Structures”
- Xavier Viegas, D., Figueiredo Almeida, M., e Ribeiro, L.M. (2019), “Análise dos Incêndios Florestais Ocorridos a 15 de outubro de 2017”, Centro de Estudos sobre

Incêndios Florestais: <https://www.portugal.gov.pt/download-ficheiros/ficheiro.aspx?v=b8567e4b-c18e-47ba-b5ac-71053d630e7f>.

ANNEX A

Duet 2 Wifi

This is the latest PCB revision of the Duet 2 Wifi, v1.04.

Duet 2 Wifi is an advanced 32 bit electronic controller for 3D printers and other CNC machines. It has the same features as the [Duet 2 Ethernet](#) other than providing WiFi connectivity rather than ethernet. [Full feature description is available in our documentation](#): in summary:

- Powerful 32 Bit Processor
- Dedicated Wifi module with either :
 - a compact built-in antenna
 - a external antenna for extending Wifi range or allowing the Duet 2 Wifi to be mounted in a shielding enclosure with the antenna outside.
- Super quiet TMC2660 stepper drivers, up to 256 microstepping.
- High speed uSD card and support for a second external SD card if required.
- Dual extruders on the main board, up to 5 more extruders on the [expansion board](#).
- High Power rating: Each stepper driver is capable of 2.8A motor current, currently limited in software to 2.4A. The bed heater channel is specifically designed for high current (18A).
- Connect via PC, tablet or smartphone on the same network to the on board web interface.
- Set up your printer and update the firmware through the [web interface](#).
- All common 3D printer geometries are supported
- Expandable up to 7 extruders with Firmware support for mixing nozzles and remapping axes to use high power external drivers.
- Support for the [PanelDue](#): a full colour graphic touch screen
- Support for [DC42's IR Z probe](#) and the [Duet3D Smart Effector](#) for delta printers.
- Provided with Molex compatible plugs and crimps as well as ferrules for power and heater terminals.

The Duet 2 Wifi can have [Thermistors](#) connected directly, alternatively we have two different temperature sensing daughterboards available:

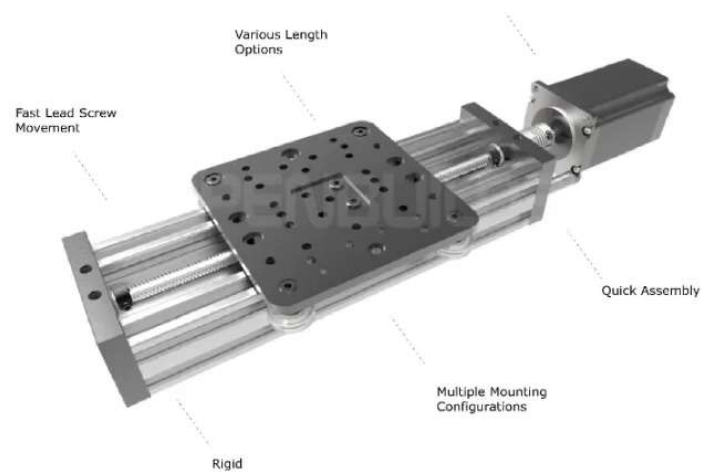
- [PT100 Temperature daughterboard](#)
- [Thermocouple temperature daughterboard](#).

We also supply genuine e3d PT100 and thermocouple sensors compatible with their range of hotends:

- [PT100 sensor](#)
- [Type K Thermocouple sensor](#).

We aim to ship all component orders received the following working day. We recommend you use one of our resellers if there is one in or near your country - see the "More Information" section lower on this page for link to resellers.

Figure A.1. DUET 2 Wifi Technical Specifications.



With strength, accuracy and power this actuator is a great choice for your projects.

It includes a wide stance, rigid gantry cart along with high resolution screw driven power.

The included gantry cart is capable of being mounted 90 degrees to each other creating either an X/Y system or even an X/Z system for a CNC machine.

This powerful actuator has the capability to get your projects moving. Get yours today!

Specifications:

- Lead Screw Driven
- Travel distance:
 - 250mm is ~4.5" (115mm)
 - 500mm is ~14" (365mm)
 - 1000mm is 35" (885mm)
- Accuracy: 0.001" ~0.003" (0.05mm ~0.10mm)
- Accuracy Positioning: 0.026mm
- Max Force: 26lb (115N)
- Max Speed: 8000 mm/min

Figure A.2. C-Beam XL Nema 23 Technical Specifications.

Desempenho	
Nível de ruído (velocidade alta)	19 dB
Velocidade de rotação (máx.)	2000 RPM
Modelo	Ventoinha
MTBF	50000 h
Diâmetro do ventilador	12 cm
Máxima velocidade de centrifugação	2000 RPM
Adequado para	Pasta de computador
Pressão máxima do ar	2,94 mmH2O
Pesos e dimensões	
Altura da Unidade	120 mm
Largura do produto	120 mm
Profundidade da Unidade	25 mm
Profundidade da caixa	327 mm
Altura da caixa	26 mm
Largura	227 mm
Peso do produto	116 g
Design	
Cor da caixa	Preto, Azul
Iluminação	LED
Conformidade com RoHS	Sim
Cor de iluminação	Azul
Gestão de energia	
Corrente nominal de linha	0,5 A
Consumo de energia	4,2 W
Voltagem	12

Figure A.3. COOLER MASTER - Sickle Flow 120mm Blue LED Fan Technical Specifications.

PMT24V350W1AK - Fonte Alimentação Industrial 24V 350W 14.6A

Manufacturer: Delta Electronics

Series: PMT

Part Status: Active

Type: Enclosed

Number of Outputs: 1

Voltage - Input: 90 ~ 132 VAC, 180 ~ 264 VAC

Voltage - Output 1: 24V

Voltage - Output 2: -

Voltage - Output 3: -

Voltage - Output 4: -

Current - Output (Max): 14.6A

Power (Watts): 350W

Applications: ITE (Commercial)

Voltage - Isolation: 3kV

Efficiency: 87%

Operating Temperature: -10°C ~ 70°C (With Derating)

Features: Adjustable Output

Mounting Type: Chassis Mount

Size / Dimension: 8.46" L x 4.53" W x 1.97" H (215.0mm x 115.0mm x 50.0mm)

Minimum Load Required: -

Approvals: CB, CCC, CE, cURus, TUVgs

Figure A.4. DELTA PMT24V350W1AK Technical Specifications.

Description:**.Item Name:**

Input voltage:4.5-35V

Output voltage: 1.5-35V(Adjustable)

Output current: Rated current is 2A,maximum 3A(Additional heatsink is required)

Features:

Conversion Efficiency: Up to 92% (output voltage higher, the higher the efficiency)

Switching Frequency: 150KHz Rectifier

Non-Synchronous Rectification Module Properties

Non-isolated step-down module (buck) Short Circuit Protection

Current limiting, since the recovery

Operating Temperature: Industrial grade (-40 to +85) (output power 10W or less)

Full load Temperature rise: 40

Load Regulation: $\pm 0.5\%$ Voltage Regulation: $\pm 2.5\%$

Dynamic Response speed: 5% 200uS

Dimension: 43*20*14mm (L*W*H)

Figure A.5. ITEAD MX130731002 Step Down Converter Technical Specifications.

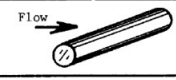

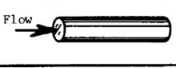
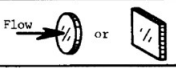
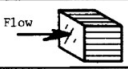
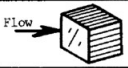

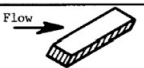

SHAPE	SKETCH	C_D
Right Circular Cylinder (long rod), side-on		1.20
Sphere		0.47
Rod, end-on		0.82
Disc, face-on		1.17
Cube, face-on		1.05
Cube, edge-on		0.80
Long Rectangular Member, face-on		2.05
Long Rectangular Member, edge-on		1.55
Narrow Strip, face-on		1.98

Figure A.6. Drag Coefficient table.

APPENDIX A

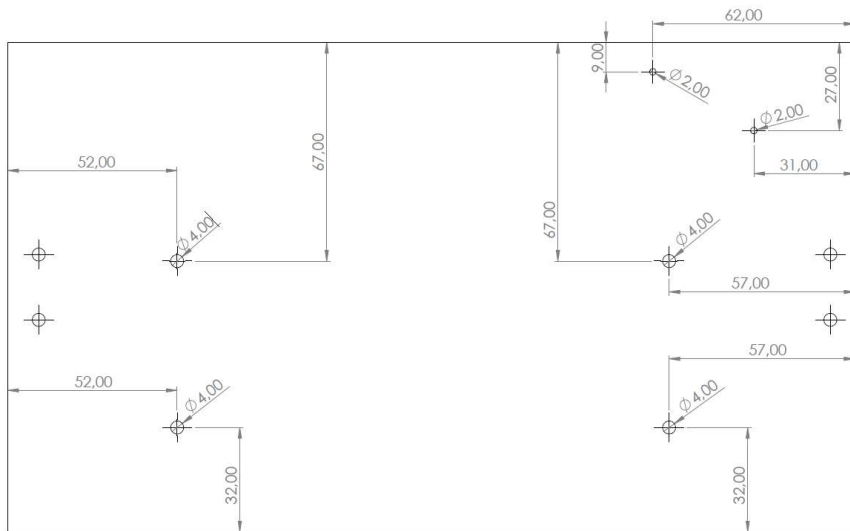


Figure Ap.1. 2D drawing of the aluminum support plates for the Power Supply and the step down converter.

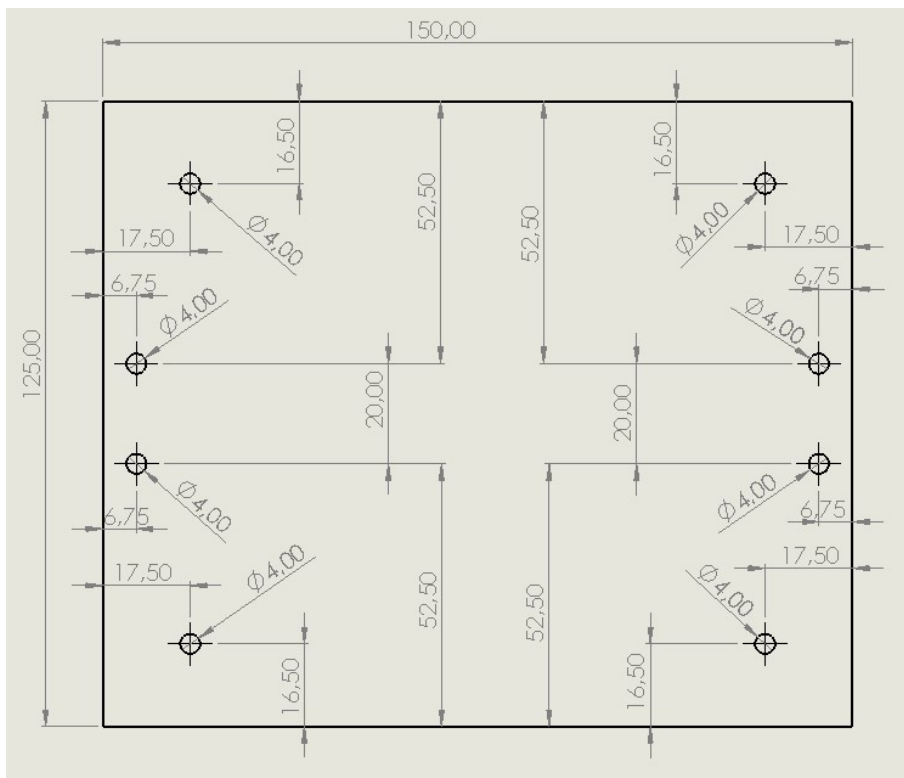


Figure Ap.2. 2D drawing of the aluminum support plates for the Controller Board.

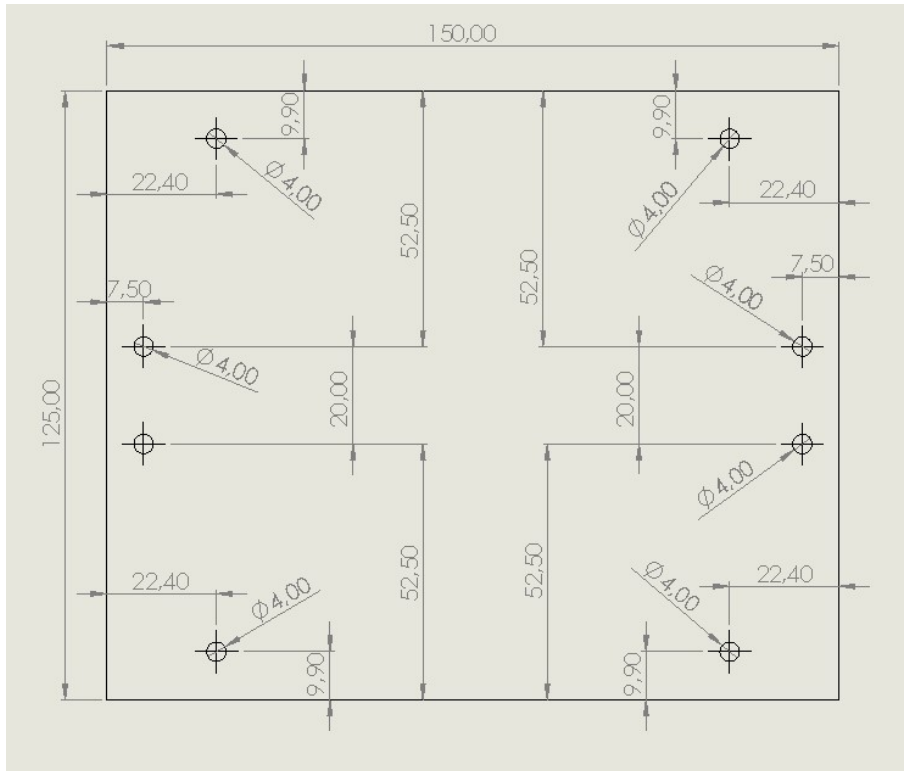


Figure Ap.3. 2D drawing of the aluminum support plates for the Cooling Fan.

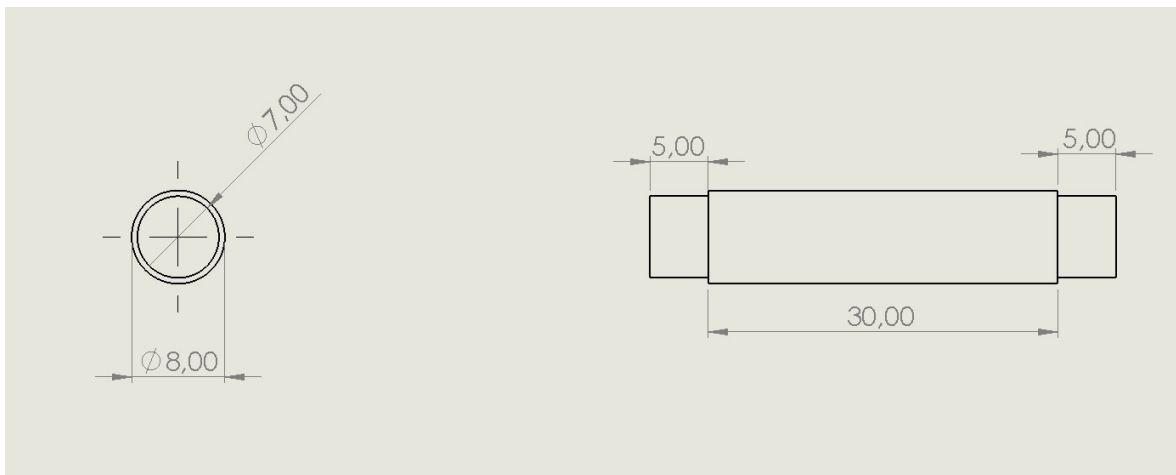


Figure Ap.4. 2D drawing of the axles for the wheels.